Magnetostratigraphic constraints on relationships between evolution of the central Swiss Molasse basin and Alpine orogenic events

F. Schlunegger* } *Geologisches Institut, Universität Bern, Baltzerstrasse 1, CH-3012 Bern, Switzerland*
A. Matter

D. W. Burbank *Department of Earth Sciences, University of Southern California, Los Angeles, California 90089-0740*

E. M. Klaper *Geologisches Institut, Universität Bern, Baltzerstrasse 1, CH-3012 Bern, Switzerland*

ABSTRACT

Magnetostratigraphic chronologies, together with lithostratigraphic, sedimentological, and petrological data enable detailed reconstruction of the Oligocene to Miocene history of the North Alpine foreland basin in relation to specific orogenic events and exhumation of the Alps. The Molasse of the study area was deposited by three major dispersal systems (Rigi, Höhronen, Napf). Distinguished by characteristic heavy mineral suites, conglomerate clast populations, and the presence of key clasts, these systems record three major phases of denudation of the Alpine edifice. The Rigi system eroded the Austroalpine and Penninic nappes of eastern Switzerland from 30 to 25.5 Ma as a result of backthrusting and uplift of these units along the Insubric Line. Subsequent uplift of the Aar massif some 40 km to the north appears to have controlled the duration of the Höhronen and Napf dispersal systems, spanning 24–22 Ma and 21.5–15 Ma, respectively. They record downcutting into the crystalline cores of the Penninic and Austroalpine nappes of eastern (Höhronen) and western (Napf) Switzerland. High-resolution reconstruction of the structural and geometrical evolution of the proximal Molasse reveals in-sequence and out-of-sequence thrusting events at the Alpine front and incorporation of the Molasse into the orogenic wedge by in-sequence thrusting and underplating. Furthermore, it reveals close relationships between periods of rapid denudation in the central Alps and phases of increased sediment accumulation rates at the proximal basin border. An initial increase in Molasse accumulation rates to >1 km/m.y. occurred between 30 and 25.5 Ma and coincides with the Insubric phase of backthrusting along the eastern Insubric Line, where >10 km of vertical displacement is interpreted. During the same time span, the Alpine wedge propagated forward along the basal Alpine thrust, as indicated by the coarsening- and thickening-upward megasequence and by occurrence of bajada fans derived from the Alpine border. The end of this tectonic event is marked by a basinwide unconformity, interpreted to have resulted from crustal rebound after initial loading. A subsequent increase in accumulation rates to >1 km/m.y. between 23 and 21.5 Ma coincides with initial uplift of the eastern Aar massif by at least 4 km. This phase of high accumulation rates is associated with incorporation of early Chattian conglomerates into the orogenic wedge. The third advance of the Alpine wedge between 21 and 15.5 Ma caused underplating of Molasse deposits, resulting in synsedimentary backthrusting of previously deposited Molasse sequences and in the development of a progressive unconformity. A rapid increase in accumulation rates from 0.35 to >1 km/m.y. between 15.5 and 15 Ma marks the final loading event in the wedge, which may be caused by further major displacement and loading of the Aar massif. This deformation is coeval with out-of-sequence thrusting of the Helvetic border chain and of the piggyback stack of North Penninic and Ultrahelvetic Flysch nappes along the basal Alpine thrust.

INTRODUCTION

Foreland-basin sequences potentially contain a decipherable record of the tectonic history of the bounding mountain belt, because the stratigraphy within the basin is controlled mainly by the development of the thrust wedge system through time (Beaumont, 1981; Jordan, 1981). Because chronologies are better established in sedimentary basins than in the adjacent fold-and-thrust belt, abundant stratigraphic research has been done in foreland basins to assess the evolutionary processes of the orogenic thrust wedge (Jordan et al., 1988; Burbank et al., 1986; Burbank et al., 1992; Colombo and Vergés, 1992). Despite a more complete and better dated record within a foreland, the correlation of sedimentary events recorded in the foreland with tectonic events in the adjacent hinterland is commonly speculative, because direct physical stratigraphic and structural ties between these areas have been removed by subsequent erosion. This is certainly the case for past studies of the Oligocene to Miocene Swiss Molasse basin, on the northern side of the Alpine orogenic wedge, where there have been several attempts to relate foreland basin stratigraphy to orogenic evolution of the adjacent hinterland (Pfiffner, 1986; Homewood et al., 1986; Sinclair et al., 1991; Sinclair and Allen, 1992). Construction of coarse-grained alluvial fans, for instance, has been attributed to hinterland uplift, whereas deposition of finer grained material has been considered to reflect tectonic quiescence. This is, however, exactly opposite to the signature that is predicted for the medial (and more commonly preserved) parts of foreland basins. Because lithofacies variation is a function of subsidence, source-area lithology, and position within the foreland, reconstruction of external controls based on sedimentary facies alone is misleading.

The first reconstruction of the structural and stratigraphic evolution of the northern Alpine foreland was made on a section in eastern Switzerland (Pfiffner, 1986; Sinclair et al., 1991). Poor time control, however, has hindered the reconstruction of the causal relationships among basin subsidence, facies evolution, and unroofing history of the Alpine wedge.

We used high-resolution magnetostratigraphy to calibrate the sedimentary, structural and geo-

*E-mail address: fritz@geodyn.psu.edu

GSA Bulletin; February 1997; v. 109; no. 2; p. 225–241; 12 figures.

metrical evolution of the proximal Molasse basin in a section across central Switzerland. On the basis of detailed temporal control, we discuss here the subsidence history and the relationships between Alpine orogeny and foreland-basin evolution. We assess timing of individual thrusting events at the tip of the orogenic wedge using the detailed chronologic record of the Molasse strata. We also focus on determining the conglomerate populations and the heavy-mineral composition of sandstones in order to identify dispersal systems within the detailed temporal framework. Finally, we attempt to identify the catchment areas and their orographic evolution as a function of orogeny.

GEOLOGIC SETTING

In the North Alpine foreland basin five lithostratigraphic units are distinguished, for which the conventional German abbreviations are used in this paper (Matter et al., 1980; Keller, 1989; Sinclair et al., 1991; Fig. 1): North Helvetic Flysch (NHF), Lower Marine Molasse (UMM), Lower Freshwater Molasse (USM), Upper Marine Molasse (OMM), and Upper Freshwater Molasse (OSM). The Molasse deposits form two coarsening-, thickening-, and shallowing-upward megasequences. The first megasequence begins with Lutetian to Priabonian NHF and with the Rupelian UMM, which are followed by the Chattian and Aquitanian fluvial clastic rocks of the USM. The second megasequence, starting with the Burdigalian transgression, consists of shallow marine sandstones (OMM), which interfinger with major fan deltas adjacent to the thrust front (Berli, 1985; Keller, 1989; Hurni, 1991). This megasequence ends with Serravalian fluvial clastic rocks of the OSM.

The study area, located in central Switzerland (Fig. 1), is a classic region of Molasse strata research. Good exposures and three deep boreholes provide detailed knowledge on lithostratigraphy and structure (Kopp et al., 1955; Matter, 1964; Gasser, 1966, 1968; Lemcke et al., 1968; Stürm, 1973; Schlanke, 1974; Vollmayr and Wendt, 1987; Ottiger et al., 1990; Greber et al., 1994). The Molasse strata of central Switzerland includes both southernmost Plateau Molasse and Subalpine Molasse (Fig. 1). The sedimentary sequence of the Plateau Molasse in this region is made up of the USM, OMM and OSM, and ranges in age from Chattian to Langhian (Figs. 2, 3A). The generally flat lying Plateau Molasse has been affected by a south-vergent backthrust owing to underthrusting of a stack of imbricate USM thrust slices (Triangle Zone, Fig. 3B; Vollmayr and Wendt, 1987). The Subalpine Molasse consists of Lower Marine Molasse (UMM) and Lower Freshwater Molasse (USM), which build the thick Rigi thrust sheet adjacent to the Alpine border. The Subalpine Molasse itself is overlain by the Helvetic nappes, and structural unconformities separate the Molasse thrust sheets from the Helvetic border chain (Haus, 1937; Scherer, 1966; Haldemann et al., 1980).

Four representative sections (Rigi, Höhronen, Fischenbach, Napf) were measured for analysis of facies, paleoflow directions, petrofacies, and magnetostratigraphy (Fig. 3A). They enable reconstruction of a synthetic north-south–oriented cross section encompassing the time range from Rupelian to Langhian (Fig. 2).

The ≈4-km-thick Rigi section, located in the Subalpine Molasse, comprises three units consisting of early Chattian proximal, alluvial fan conglomerates with few fine-grained facies (Stürm, 1973). This succession, which is dominated by carbonate rock fragments in both conglomerates and sandstones, is referred to as USM I (Schlanke, 1974).

The Höhronen section consists of a 300-m-thick Aquitanian alternation of sandstones and mudstones in the lower part (unit A), followed by a predominantly conglomeratic succession 1100 m thick (unit B, Höhronen conglomerate) and an alternating series of conglomerates, sandstones, and marls ≈500 m thick (unit C).

A partly contemporaneous distal sequence comprising a 750-m-thick alternation of fluvial

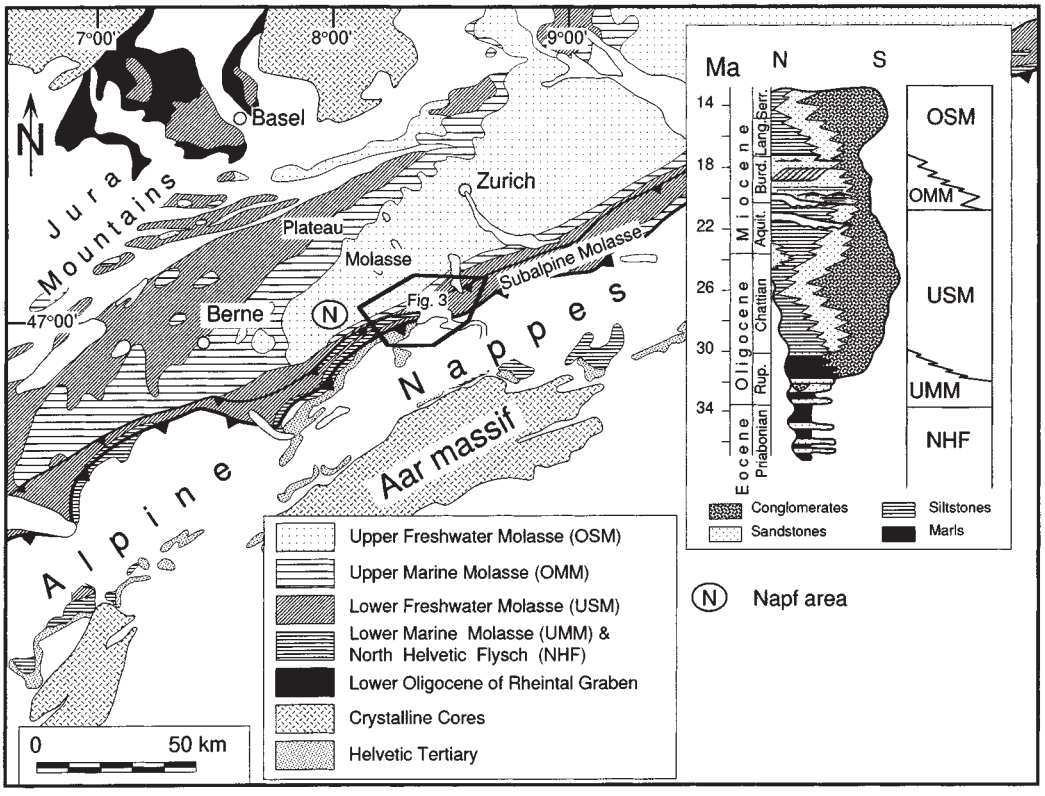

Modified after Keller et al. (1990)

Figure 1. Geological map of the Oligocene–Miocene Swiss Molasse basin and the adjacent Alpine orogen, with location of the study areas and general stratigraphy of the foreland basin (modified after Schlunegger et al., 1996).

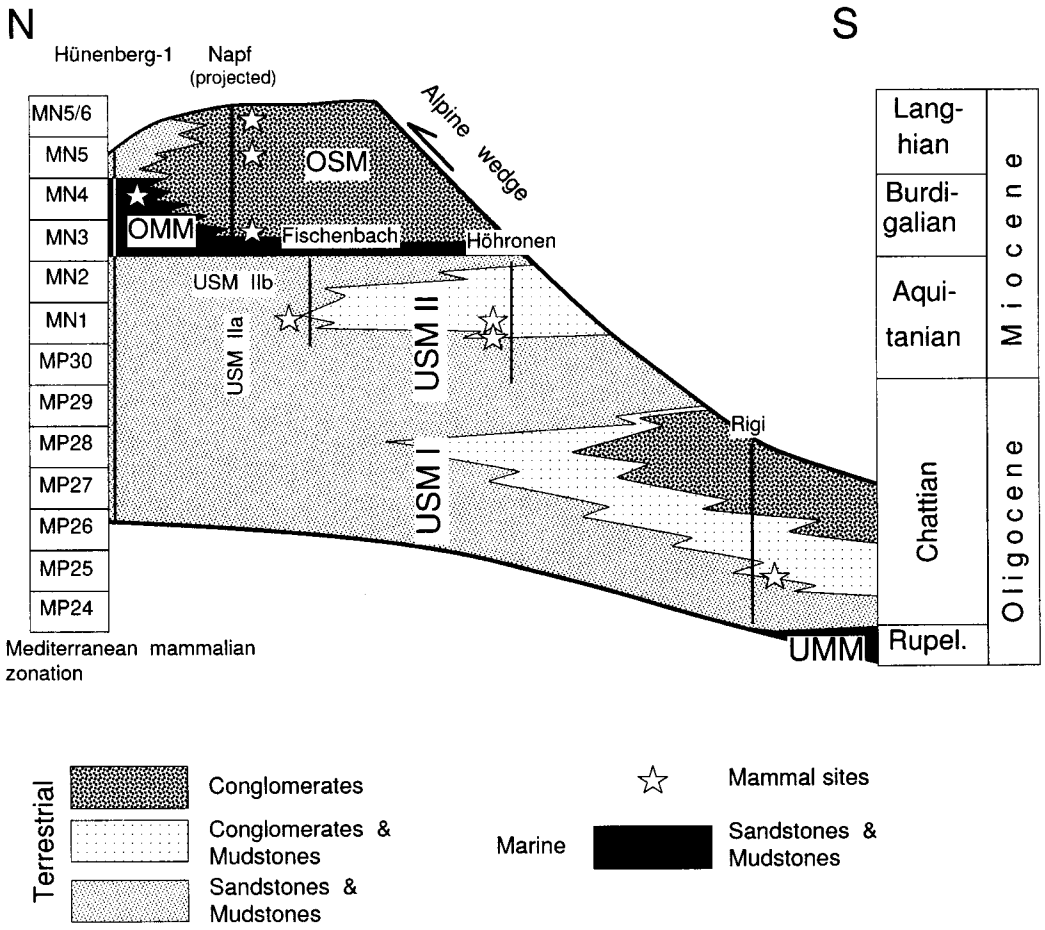

Figure 2. Synthetic chronostratigraphic (Wheeler) diagram of the proximal Molasse of central Switzerland. The analyzed sections and their approximate time span are marked by solid lines. The Mediterranean mammalian zonation is taken from Engesser (1990), with modifications by Mödden and Gad (1992) and Mödden (1990).

channel sandstones and overbank fines is represented by the Fischenbach section in the upturned Plateau Molasse (Gasser, 1966; Schlunegger et al., 1996). The Fischenbach and Höhronen sections constitute the USM II of Schlanke (1974), which is characterized by the low carbonate and high feldspar content of its sandstones as well as by the presence of the key heavy minerals apatite and zircon in the lower part (USM IIa) and epidote in the upper part (USM IIb, Gasser, 1966; Müller, 1971; Schlanke, 1974).

The Napf section is located 40 km west of the study area in the Napf alluvial fan. It consists at the base of 100 m of OMM overlain by a succession of OSM more than 1400 m thick (Matter, 1964), ranging in age from Burdigalian to Langhian (Keller, 1989; Hurni, 1991), or approximately 19 to 15 Ma, according to recent magnetostratigraphic calibration (Schlunegger et al., 1996). Here, the OSM is partly contemporaneous with the OMM (Hurni, 1991). The OSM consists of fluvial fining-upward cycles dominated by conglomerates.

The well Hünenberg-1 explored an undisturbed sequence of the entire Plateau Molasse down to the Mesozoic basement (Lemcke et al., 1968). The USM rests directly on upper Jurassic limestones and is composed of carbonate-rich sandstones and siltstones (USM I) overlain by alternating arkoses and mudstones (USM II).

METHODOLOGY

Each stratigraphic section was measured by using a Jacob's staff and Abney level. The sections were divided into large-scale facies associations that were mapped at a scale of 1:25 000, making use of previously published geological maps.

Paleocurrents were determined from furrows, large-scale (>0.5 m) trough cross-beds, and imbricate clasts in the conglomerates. The tectonic tilt in the Subalpine Molasse was removed in order to determine the paleoflow direction at the time of deposition. Conglomerate compositions were determined every 100 m on 200 clasts with a long diameter >2 cm collected from 1 m^2 of outcrop. Moreover, special attention was given to the first appearance of distinctive clasts. In addition, using the method described by Schlunegger et al. (1993), 37 heavy mineral analyses were carried out on cuttings from the Hünenberg-1 well.

For magnetostratigraphy, brown to yellowish laminated or massive mudstones and siltstones were preferentially sampled (for sample location maps, refer to Schlunegger, 1995). An individual sample strategy had to be chosen for each section dependent on availability of mudstones and siltstones, biostratigraphically defined time span, and expected number of reversals. At the top of the Rigi section, fine-grained rock types are sparse, and samples were collected every 50–100 m. Four to five oriented samples were taken for each site, and bedding orientation was measured for tilt correction. Detailed thermal and alternating field demagnetization analysis of specimens from different parts of the basin and different depositional systems revealed the presence of three to four magnetic components (Burbank et al., 1992; Schlunegger et al., 1996): (1) a low-temperature magnetic signal, removed at 250 °C, which is probably carried by titanomagnetite minerals, (2) a magnetic signal in the 250–550 °C temperature window related to magnetite group minerals, (3) a magnetization remaining at high temperatures, most probably carried by hematite crystals, and (4) occasionally sulfide minerals. These pilot studies showed that specimens containing titano-

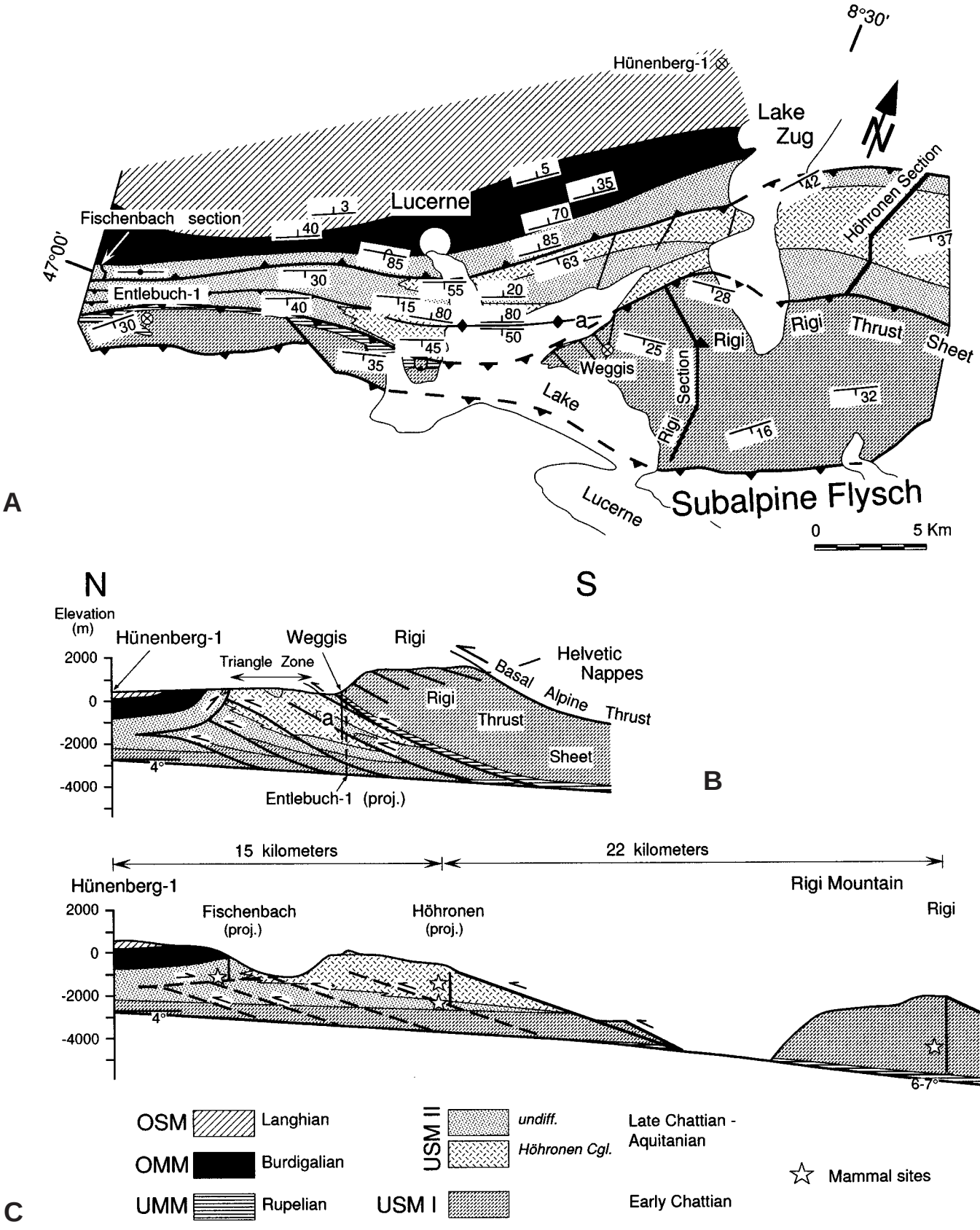

Figure 3. The central Swiss Molasse basin with (A) a compilation of geologic maps (Kopp et al., 1955; Gasser, 1966, 1968; Matter, 1964; Stürm, 1973; Schlanke, 1974; Ottiger et al., 1990), (B) cross section, and (C) palinspastic restoration.

magnetite, magnetite, and hematite minerals reveal reliable characteristic remanent magnetizations (CRMs) within the 250–550 °C temperature window, and that magnetic directions in the lower and upper temperature windows are unstable and of opposite and mixed polarities. However, organic-rich rock types, which are prone to contain sulfide minerals, displayed stable demagnetization vectors within a 250–350 °C temperature window. On the basis of these pilot studies, Schlunegger et al. (1996) concluded that (1) despite the possible postdepositional growth of titanomagnetite, sulfide, and hematite crystals, the intensities of these secondary mineral phases are too weak to have a significant influence on the CRM of the samples; and (2) reliable CRMs are detected in the 250–350 °C window for all fine-grained rock types of the Molasse basin. Therefore, on the basis of this conclusion, all specimens were demagnetized at 250, 300, and 350 °C in this study. The coherence of the magnetic directions of each site was tested by using Fisher (1953) statistics. Sites were classified as class I if three samples were grouped with $k \geq 10$. They were classified as class II if $k < 10$ for three samples and $k \geq 10$ for two samples. The mean magnetic vector of each site was used to calculate the virtual geomagnetic pole (VGP; Fisher, 1953). The latitude of the VGP formed the basis for the local magnetopolarity stratigraphy (MPS). Additionally, an α_{95} error envelope was calculated for each VGP latitude. The chronology of Schlunegger et al. (1996), which calibrates the Molasse groups of central Switzerland and the Mediterranean mammalian assemblage zonation of Engesser (1990), Mödden and Gad (1992), and Mödden (1993) is used as reference for correlating the MPS with the global magnetic polarity time scale (MPTS) of Cande and Kent (1992, 1995). The MPSs of the analyzed sections were correlated to the MPTS through (1) consideration of index fossils (mammalian fauna), (2) recognition of distinctive reversal patterns, and (3) consideration of regional lithostratigraphy.

A tectonostratigraphic balanced cross-section of the proximal Molasse basin was constructed by using a compiled geologic map and subsurface data from deep wells. A palinspastic restoration of this section was made in order to establish the amount of shortening and to determine the basin geometry and the original facies patterns through time.

RESULTS

Five sections on a palinspastically restored cross section reported here give insights into the evolution of the shape of the basin, the facies architectures, and the dispersal systems as a response to orogenic events in the Alpine hinterland. The detailed magnetostratigraphies chronicle the changes of the depositional environments and basin subsidence. These record four thrusting events at the Alpine front and indicate incorporation of Lower Freshwater Molasse (USM) into the orogenic wedge as early as 23 Ma.

Structure and Palinspastic Restoration

The structural style of the Subalpine Molasse in the Lake Lucerne area is characterized by a lateral change from a thrust belt to a fold-and-thrust belt. In addition, in this area the strike of the basal Alpine thrust is discordant to the bedding of the underlying Rigi thrust sheet (Fig. 3A).

The north-south tectonostratigraphic section (Fig. 3B) is based on (1) the geological and structural data shown in Figure 3A and (2) three deep wells that constrain the depth of the Mesozoic basement, the location of thrust planes, and—together with the measured sections—the thicknesses of the individual lithostratigraphic units. These data reveal a dip angle of 4° for the top of the Mesozoic basement and suggest that the main decollement horizon lies within the basal Molasse sequence. Moreover, the wells and field data indicate decreasing thicknesses of UMM, USM I, and USM II (inclusive of the Höhronen conglomerate) away from the Alpine front. The USM I shows the most significant change in thickness from at least 3600 m at Rigi Mountain to ≈450 m in the Hünenberg-1 and Entlebuch-1 wells (Lemcke et al., 1968; Vollmayr and Wendt, 1987), indicating, as discussed herein, that the dip angle of the Mesozoic basement had to change through space and time as a response to ongoing thrust wedge advance (see also Fig. 3). The anticline in the Triangle Zone (labeled as "a" in Fig. 3, A and B) is interpreted as a fault-propagation fold with a blind thrust in its core which reaches the surface west of Lake Lucerne. The amount of shortening in the Triangle Zone is on the order of ≈7 km, which is 9 km less than postulated by Burkhard (1990). Because the thickness of USM II was previously underestimated (Burkhard, 1990), greater thrust displacements of USM I were previously required to balance the section within the triangle zone. A minimum of 12 km is necessary to restore the Rigi thrust sheet. However, the total amount of shortening for the Molasse basin–Jura Mountains systems is on the order of 30 km, on the basis of seismic data (Pfiffner et al., 1996a), which includes 6 km of displacement for the Jura Mountains, according to Matter et al. (1988a). These data suggest that ≈16 km of shortening must be considered to restore the Rigi thrust sheet (Fig. 3C).

A progressive unconformity appears to be present in the backthrust part of the Plateau Molasse as indicated by southward onlap of OSM on OMM reflections seen in seismic data (Schlunegger et al., in press) and southward-convergent OSM conglomerate horizons with increasingly fine-grained pebbles and cobbles toward the Triangle Zone.

Chronostratigraphy

The high sample density in the studied sections defines rather unambiguous magnetic reversal patterns. The magnetic polarity stratigraphy (MPS) of the Fischenbach and Napf sections (Fig. 4, A and B) were correlated with the magnetic polarity time scale (MPTS) of Cande and Kent (1992, 1995) by Schlunegger et al. (1996) on the basis of (1) the Ries event at 14.6 ± 0.6 Ma, postdating the top of the Napf section, (2) chemostratigraphic data of Keller (1989), and (3) comparison with magnetostratigraphies of neighboring sections. These authors calibrated the Fischenbach and Napf sections with the time span from chrons 6Cn.1 to 5C—i.e., Aquitanian to Langhian (Fig. 4C). Furthermore, they also identified and estimated the duration of unconformities within the USM and the OSM as well as at the base of the OMM.

The base of the Rigi MPS is correlated with the MPTS on the basis of (1) mammalian index fossils indicating MP25 and (2) recognition of a distinctive reversal pattern (Fig. 5A). According to Schlunegger et al. (1996), MP25 lasted from approximately 29 Ma to 27.5 Ma. However, the correlation of the long interval of normal polarity in the upper part of the section is poorly constrained. Because of the low sample density in this part of the section, reversed polarities could have been missed either at the base or the top of this long interval of normal polarity (solutions 2 and 3, Fig. 5A). Solution 3 suggests that chron 8n is represented in the Rigi section by a relatively short interval of normal polarity (Fig. 5C), which implies a hiatus at the base of unit B, given the regular pattern of reversals in the underlying unit A. However, new mapping and careful examinations of large exposures in three dimensions (Buxtorf et al., 1916) do not reveal any unconformities or onlap relationships, which are key indicators for the presence of hiatuses. We therefore reject solution 3. Solution 2 implies that the top of the Rigi section correlates either with chron 7An or 8n, which suggests that it may be as young as 25.5 Ma.

Correlation of the magnetostratigraphy of the Höhronen section (Fig. 5B) is guided by mammalian index fossils at the base and the top, which indicate MN1. Because the lower boundary of MN1 is precisely dated with chron 6Cn.1n (Schlunegger et al., 1996), the long reversed-polarity interval at the base of the Höhronen section most probably correlates with chron 6Br

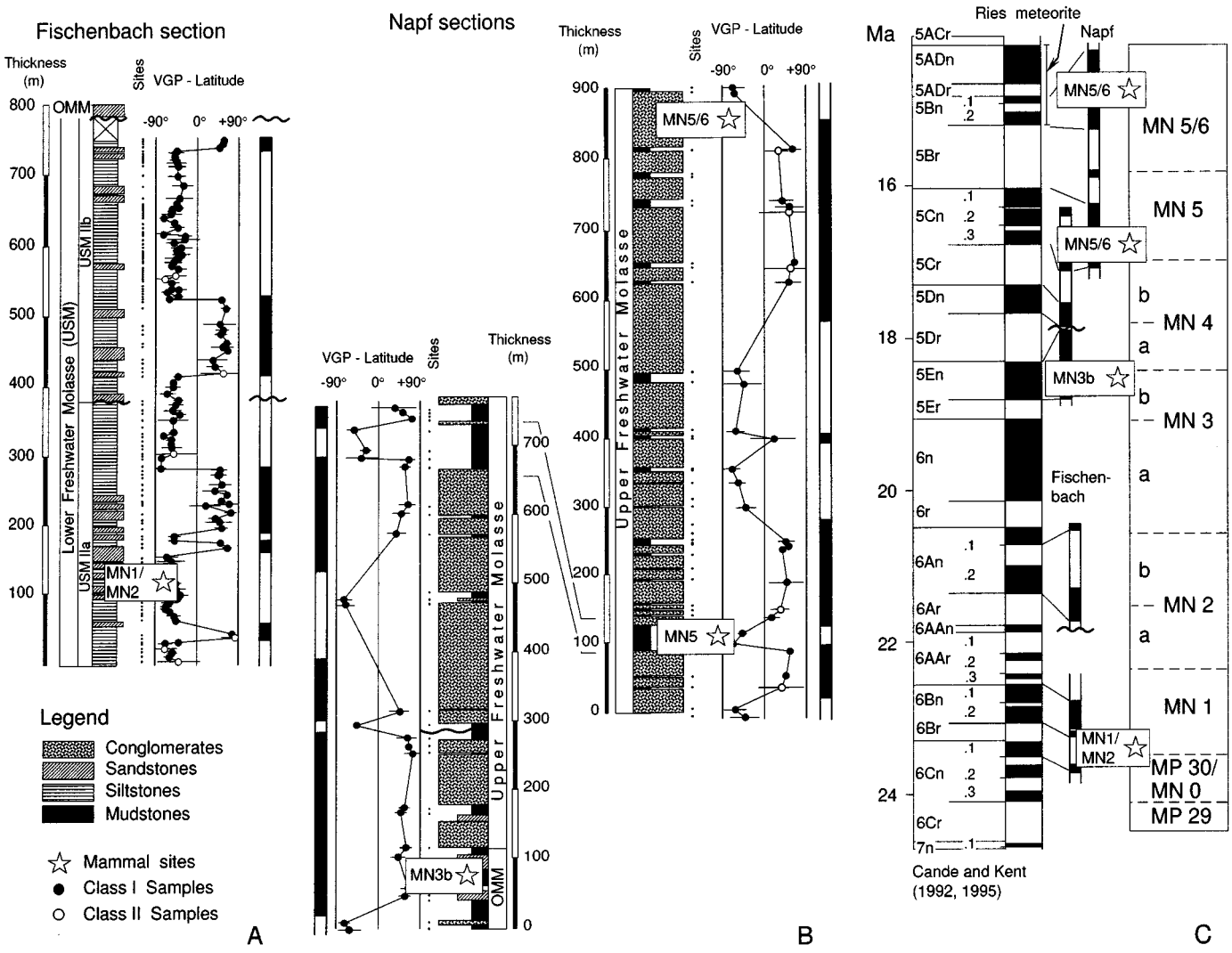

Figure 4. Magnetostratigraphy and sedimentology of (A) Fischenbach and (B) Napf sections, and (C) correlation with the magnetic polarity time scale (modified after Schlunegger et al., 1996).

(Fig. 5C). The calibration of the uppermost four reversals of the Höhronen section, however, is poorly constrained because no chronology is available to date exactly the upper boundary of MN1 (Schlunegger et al., 1996). Nevertheless, the top of the Höhronen MPS can be calibrated either with chrons 6AAr.2, 6AAr.1 or 6Ar. However, unit B of the Höhronen section contains the key heavy minerals apatite and zircon (USM IIa; Schlanke, 1974), which are replaced in the Molasse by epidote at the base of USM IIb at 21.5 Ma, at the latest (upper boundary of chron 6Ar) (Gasser, 1966; Schlanke, 1974; Schlunegger et al., 1996). Furthermore, at Höhronen, the overlying 800-m-thick alternation of conglomerates and siltstones (unit B) also contains the key heavy minerals apatite and zircon (Schlanke, 1974). Therefore, it appears most reasonable to calibrate the uppermost reversed polarity of the Höhronen section either with chron 6AAr.2 or 6AAr.1 (Fig. 5C).

No magnetostratigraphy could be established on the Hünenberg-1 well because only cuttings were available. Nonetheless, a general calibration of the sequence can be achieved through (1) lithostratigraphic correlation with the other well-dated sections shown in Figure 6, (2) seismic stratigraphy (Schlunegger, 1995), and (3) magnetostratigraphic dating of the USM-OMM and OMM-OSM boundaries within the study area (Schlunegger et al., 1996). This calibration suggests that USM I at Hünenberg-1 (Fig. 6) represents a distal facies equivalent of the conglomeratic succession cropping out at Rigi Mountain and spans approximately 28.5–25.5 Ma. The lower age limit of USM II is difficult to assess because no chronologic data are available within the study area. However, a mammalian fauna detected approximately 150 m above the base of USM II 50 km farther northeast (Matter et al., 1988b) and the magnetostratigraphic calibration of the Höhronen section indicate an age of ca. 24 Ma (Fig. 6). The upper part of USM II is correlated with the dated Fischenbach section (Fig. 6), which represents the same facies belt (Schlunegger 1995), assuming similar accumulation rates. The proposed correlation results in a hiatus of ≈1.5 m.y. for the unconformity that is seen on seismic lines between USM I and USM II (Schlunegger, 1995).

Lithofacies and Accumulation Rates

Three coarsening- and thickening-upward megasequences are preserved in the proximal Molasse of central Switzerland (Fig. 7). The lower megasequence, comprising Rupelian to early Chattian UMM and USM I, is best developed in the Rigi section. Here, a 2000-m-thick

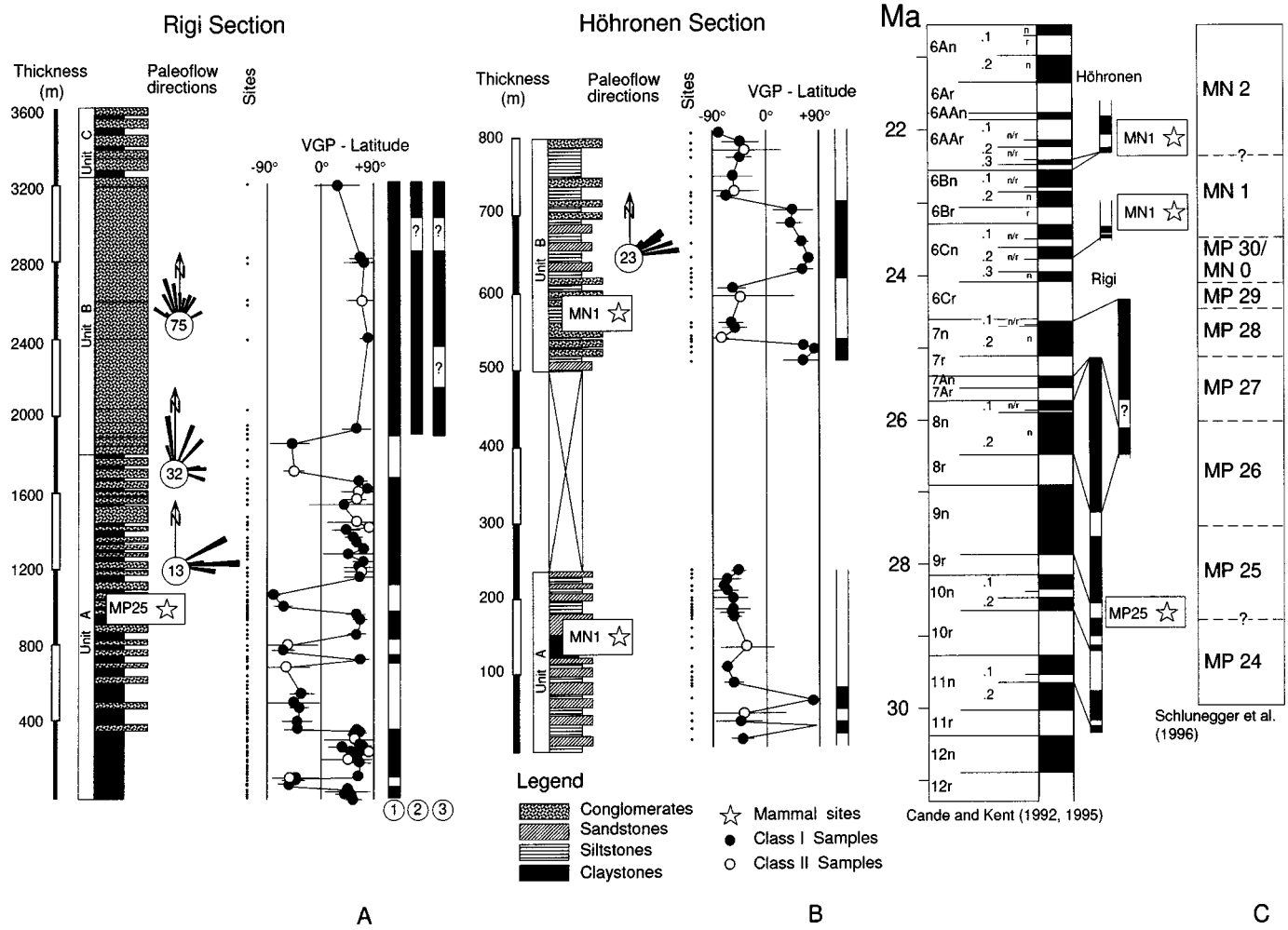

Figure 5. Magnetostratigraphy and sedimentology of (A) Rigi and (B) Höhronen sections, and (C) correlation with the magnetic polarity time scale. The magnetostratigraphic calibration of the mammal assemblage zonation is taken from Schlunegger et al. (1996). The magnetopolarity stratigraphies labeled as 1, 2, and 3 in A represent alternative solutions (refer to text for explanation).

sequence of alternating conglomerates and mudstones (unit A) is overlain by a 1300-m-thick succession of massive conglomerates (unit B), which are topped by mudstones with intercalated ribbon conglomerates (unit C), measuring 300 m (Fig. 6). The conglomerate beds of unit A are between 1.5 and 5 m thick and display a strong concave shaped erosive base with deep scours. The interbedded fine-grained sediments reveal planelamination, ripple cross-bedding, mottling, root traces, and bioturbation. The geometry and texture of the lithofacies found in unit A suggest the presence of an alluvial plain with channelized water flow. Unit B consists of massive and horizontally bedded well-sorted conglomerates with imbricated clasts. This unit is interpreted to have been deposited by sheetflood dispersion on an alluvial fan. Unit C, however, contains mottled mudstones, matrix-supported conglomerates, and 3-m-thick, deeply incised ribbon conglomerates. This unit appears to have been laid down by high concentration to hyperconcentration flows. Furthermore, mapping reveals that unit C encroaches laterally onto the alluvial fan. This geometrical relationship suggests that the conglomerates and mudstones of unit C were deposited on local (bajada) fans (Schlunegger et al., 1993). Given the possible calibrations of the Rigi section as discussed previously herein (Fig. 5C), the facies evolution from the base to the top of the Rigi section is associated with a steady increase in accumulation rates, from 0.7 km/m.y. in unit A to more than 1.0 km/m.y. toward the end of fan construction. In contrast, the distal part of the basin is characterized by a low accumulation rate of <0.3 km/m.y. and by deposition of a sandstone-dominated lithofacies (Figs. 7, 8).

The intermediate coarsening- and thickening-upward megasequence postdates a hiatus of ≈1.5 m.y. and begins at ca. 24 Ma (Fig. 7). It is best developed in the Höhronen section, where ≈300 m of alternating sandstones and mudstones (unit A) are overlain by a succession of conglomerates and mudstones more than 1100 m thick (unit B) and an alternating series of conglomerates, sandstones and mudstones ≈500 m thick (unit C). Given the possible calibrations of the Höhronen section as discussed previously herein, the intermediate coarsening- and thickening-upward trend is accompanied by an increase in accumulation rates from less than 0.2 km/m.y. in unit A to >1 km/m.y. in unit B and probably unit C (Fig. 8). Farther north in the Hünenberg-1 section (Figs. 6, 7), contemporaneous successions are predominantly sandstone. In contrast to the Höhronen section, the accumulation rate at Hünenberg-1 decreases up-section from >0.5 to 0.3 km/m.y. (Fig. 8). Mapping at Höhronen reveals highly variable thicknesses and compositions of conglomerate beds in

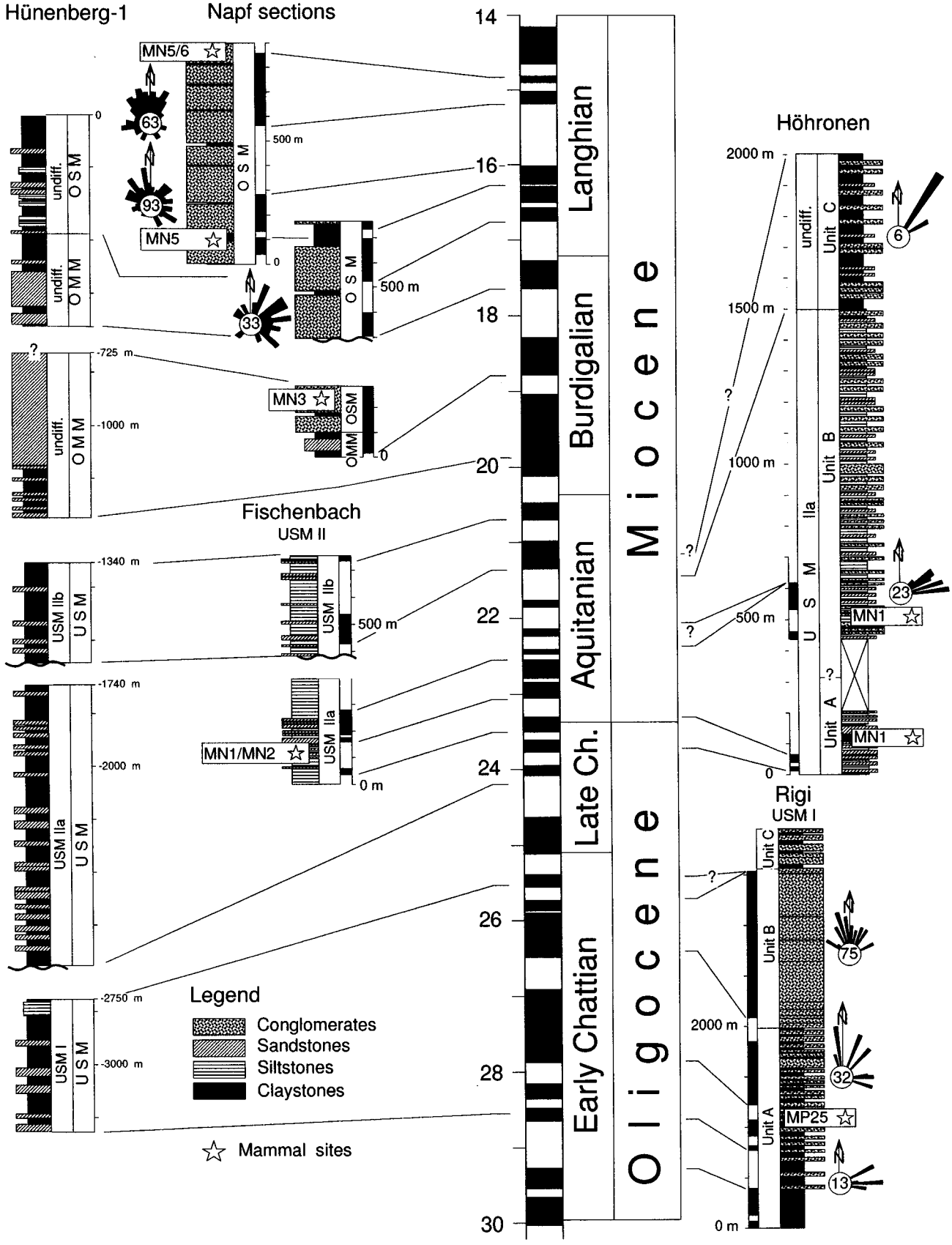

Figure 6. Correlation of the magnetopolarity stratigraphy of the studied sections with the magnetic polarity time scale of Cande and Kent (1992, 1995). The magnetostratigraphic calibration of the Molasse groups is taken from Schlunegger et al. (1996).

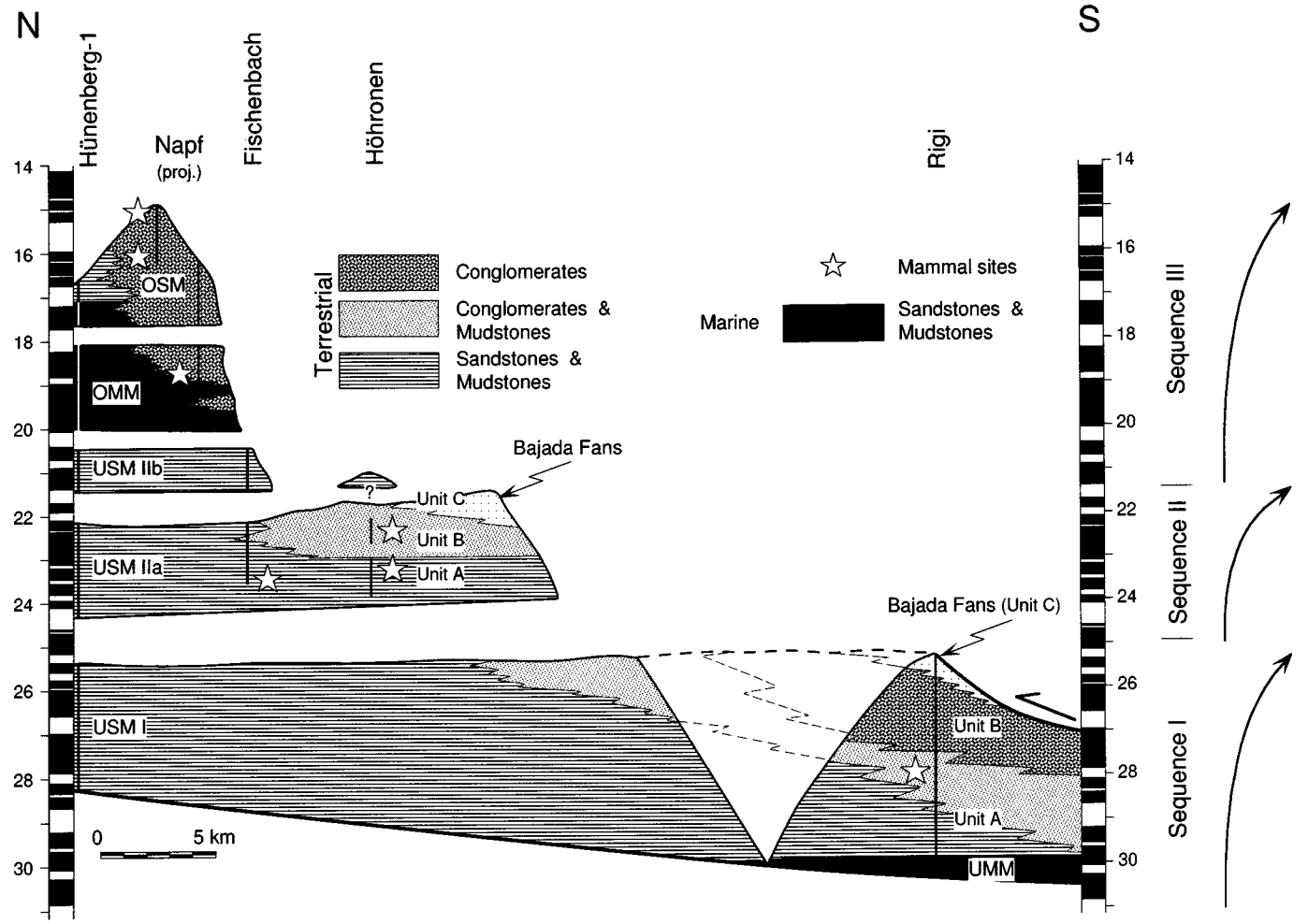

Figure 7. Chronologic (Wheeler) diagram of a palinspastically restored section across the central Swiss Molasse basin, supporting a strong heterochroneity of facies.

unit C, as well as matrix-supported conglomerates and sandstones. These are interpreted to represent deposition by rivers and hyperconcentrated flows on locally derived bajada fans (Schlunegger et al., 1993).

The upper coarsening- and thickening-upward megasequence measured in the Napf and Fischenbach sections and in the Hünenberg-1 well follows a hiatus at approximately 21.5 Ma (Fig. 7). The section comprises the whole Molasse succession from USM IIb to OSM and includes the OMM. Measuring 350 m thick, the USM IIb is made up of fining-upward fluvial sandstone-mudstone cycles. The sandstone is typically massive or trough cross-bedded, whereas the upper part of the mudstones commonly has mature paleosols. This facies association is interpreted to represent a sinuous river belt depositional system. An unconformity spanning about 0.5 m.y. in the study area lies at the base of a 950-m-thick Burdigalian succession of shallow marine sandstones. Approaching the Napf fan, these sandstone strata are progressively replaced by terrestrial deposits of the OSM up to 1400 m thick. The magnetostratigraphy established on the Napf section suggests the presence of another unconformity within the OSM. This unconformity is interpreted to result from base-level lowering during a Burdigalian regression described by Keller (1989) in the OMM and observed in seismic lines (Schlunegger et al., in press). In the time interval between 21 and 15.5 Ma, the accumulation rates continuously decreased in megasequence III, from 0.5 to 0.35 km/m.y. (Fig. 8). However, a marked increase of the accumulation rate up to a maximum value of 1.7 km/m.y. occurs in the uppermost part of the section (15.5–15 Ma).

Dispersal Systems and Provenance

The various lithofacies of the Molasse in the study area have been interpreted as the product of a broad spectrum of depositional processes including turbidity currents, tidal and wave activity (Diem, 1986; Keller, 1989), and streamflows and hyperconcentrated flows on alluvial systems. The petrofacies and lithofacies data shown in Figure 9 reveal three major (Rigi, Höhronen, Napf) and two local dispersal systems (Fig. 10).

The depocenter of the Rigi alluvial fan system is located at Rigi Mountain east of Lake Lucerne, where stacked massive conglomerates form precipitous rock cliffs. Magnetostratigraphic chronologies reveal that it was active from ca. 30 to ca. 25.5 Ma (Fig. 10). The encroachment of the Rigi fan into this area is interpreted from abrupt upward coarsening, acceleration in the sediment-accumulation rate, and a switch from axial to transverse paleocurrents (Figs. 5A, 6, and 8). The Rigi system is characterized by the presence of the key heavy minerals spinel, zircon, and apatite and by a high content of carbonate rock frag-

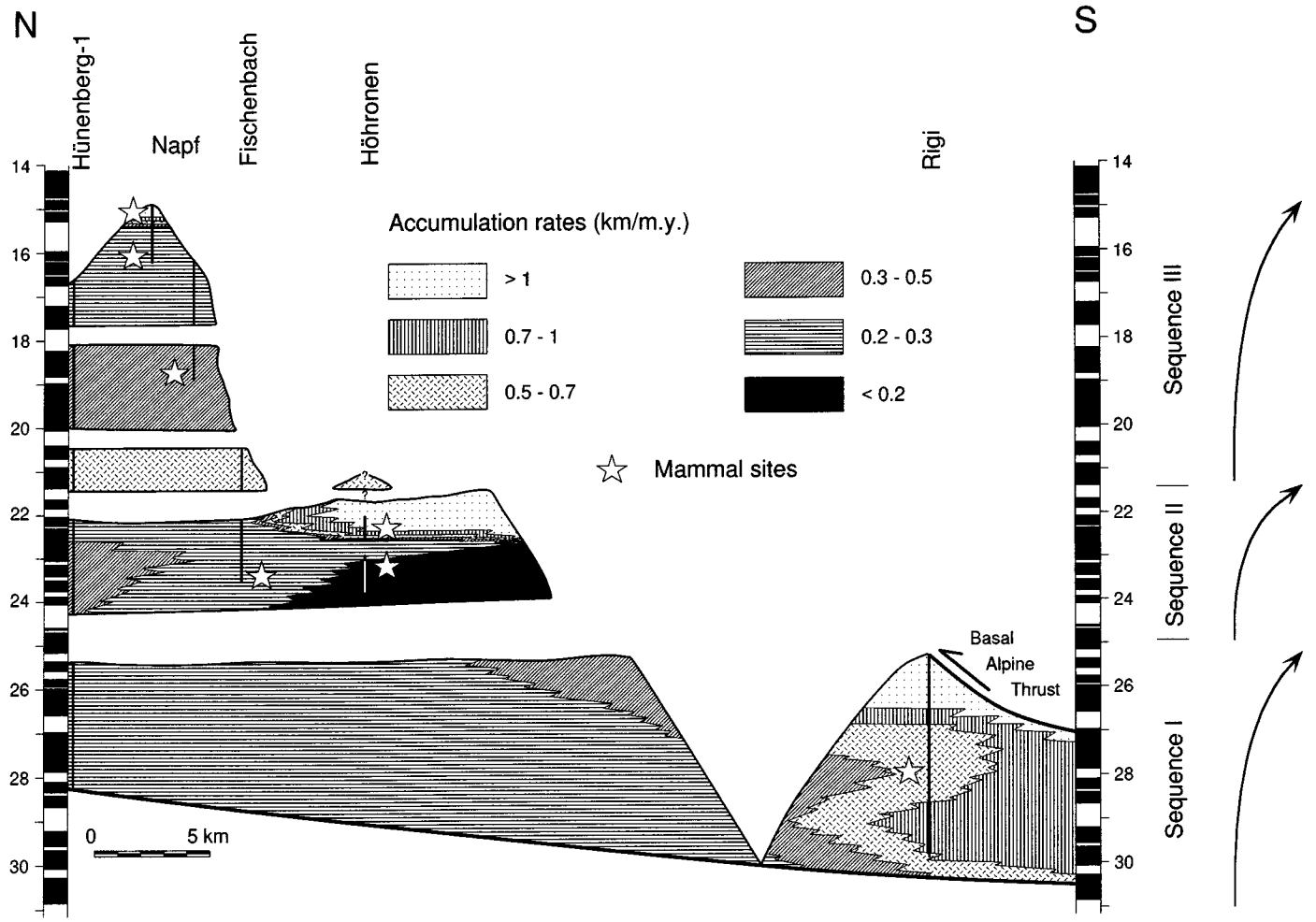

Figure 8. Palinspastically restored cross section of the central Swiss Molasse basin showing variations of decompacted sediment accumulation rates.

ments in the sandstones as well as by red granite clasts and a predominance of carbonate and flysch sandstone clasts in the conglomerates (Fig. 9). The relative frequencies of these constituents show clear trends. The high percentage of sedimentary clasts in the lower part of the section and key clasts (Müller, 1971; Stürm, 1973) suggest derivation from the sedimentary cover of the Penninic and Austroalpine nappes of eastern Switzerland. The appearance of red granite clasts and apatite in the upper part of the section, however, indicates unroofing of these nappes down to their crystalline cores. Moreover, the presence of two types of flysch sandstones (Stürm, 1973) with different heavy mineral suites characterized by spinel and apatite record erosion of South Penninic and North Penninic to Ultrahelvetic Flysch nappes, respectively (Gasser, 1967). Clasts of flysch derived from these nappes predominate in the local bajada-fan conglomerates at the top of the Rigi section. An increase in clast size in the upper part of the section and the prevalence of flysch clasts suggest increased relief and erosion of the Alpine frontal units. In the USM I of the Hünenberg-1 section, however, traces of spinel and abundant apatite and zircon, as well as a high carbonate content, are interpreted to result from deposition by early Chattian axial systems derived from farther west (Gasser, 1968; Schlunegger, 1995).

The second major alluvial system, referred to as Höhronen, was active from ca. 24 to ca. 22 Ma and is characterized by the key heavy minerals apatite and zircon (Füchtbauer, 1959; Gasser, 1966; Müller, 1971; Schlanke, 1974), (Figs. 9, 10). The conglomerate population consists of abundant crystalline clasts, mainly granites, and admixtures of sedimentary components derived from the crystalline cores and the sedimentary cover of the Penninic and Austroalpine nappes of eastern Switzerland (Renz, 1937; Kleiber, 1937; Speck, 1953; Müller, 1971). However, rare key clasts of the Rigi dispersal system such as pebbles of red granites and highly bioturbated muddy limestones also occur in the younger Höhronen conglomerates. Paleocurrent directions document a northeastward paleoflow, indicating axial drainage of the Höhronen fan (Fig. 5B). The fan apex is not exposed, but it must be located directly west of Rigi Mountain where the Höhronen fan disappears beneath the thrust plane of the Subalpine Molasse.

No systematic clast counts were carried out for the bajada fans at the top of the Höhronen section (unit C). However, new mapping reveals that unit C contains clast types identical to those found in conglomerates in units A and B of the Rigi section (see also Müller, 1971). However, a careful look at the conglomerate and sandstone composition revealed that the evolution of the petrographic composition of the bajada fan conglomerates and sandstones reveals a trend opposite to that found in the Rigi section, suggesting normal unroofing of Rigi Mountain (see also Colombo, 1994). This is supported by transverse paleoflow directions measured in unit C (Fig. 6),

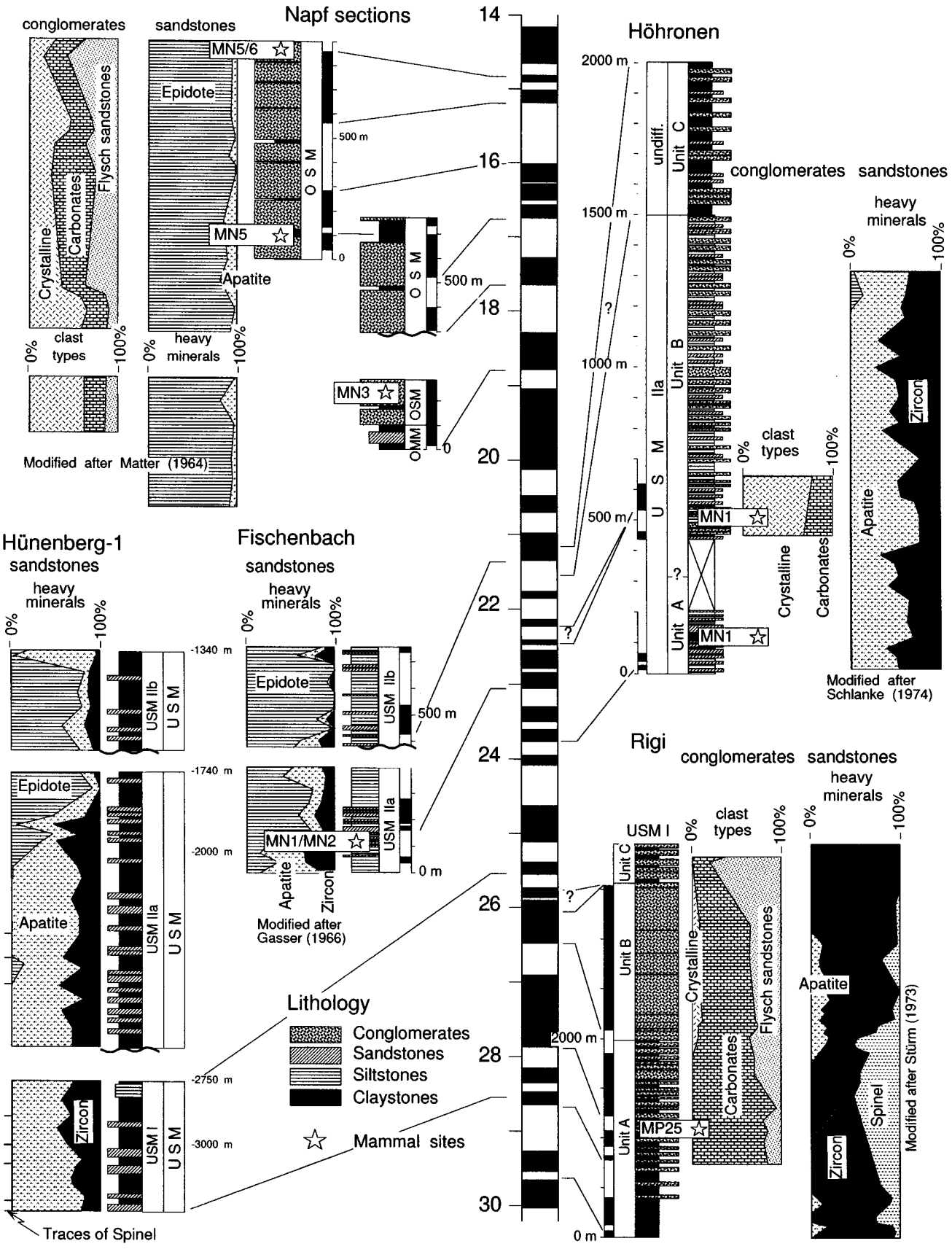

Figure 9. Schematic lithologic logs and sedimentary petrography of the studied sections, suggesting heterochroneity of petrofacies.

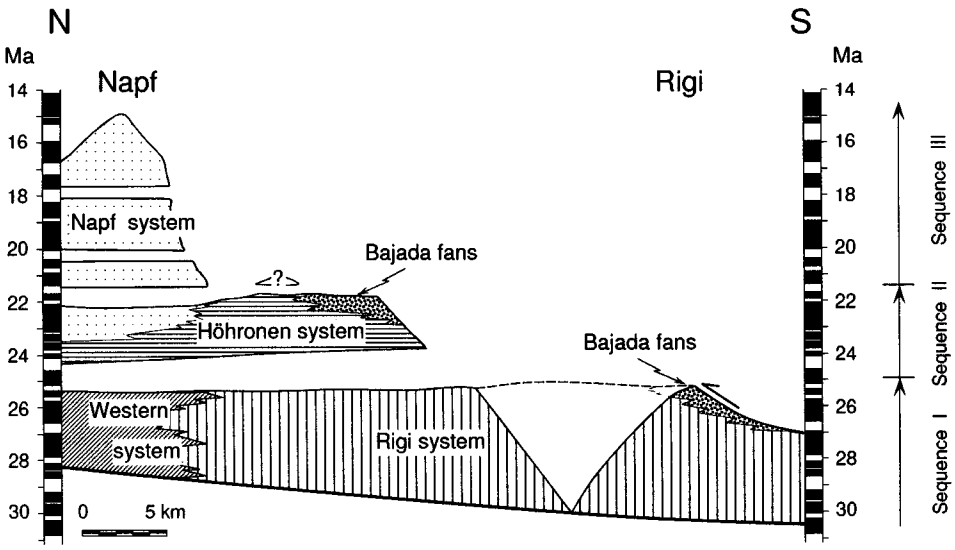

Figure 10. Chronologic (Wheeler) diagram, revealing the temporal and spatial distribution of dispersal systems. This diagram is based on the palinspastic restoration shown in Figure 3B and the calibration of petrographic units shown in Figure 9.

indicating provenance from Rigi Mountain.

Representing the third major drainage in the study area, the Napf system was active from about 21.5 to 15 Ma (Fig. 10). In contrast to the other sections, the Napf system is distinguished by a totally different petrofacies with a predominance of epidote in the heavy mineral spectrum and a change from a crystalline-dominated to a sediment-dominated conglomerate population (Fig. 9). Furthermore, in the upper part of the section the flysch clasts, mainly of Ultrahelvetic to North Penninic origin, given their heavy mineral composition, increase in abundance and size. These results and previous studies on the origin of clast types and heavy minerals (Füchtbauer, 1964; Matter, 1964) indicate that the detritus was derived from the upper Penninic and Austroalpine nappes of southwestern Switzerland. Mapping of maximum clast size distribution in relation to paleocurrent directions suggests that the fan apex was located 80 km southwest of Lucerne and indicates a change from transverse to axial drainage toward the study area (Schlunegger, 1995). However, the increasing admixture and size of flysch clasts toward the top of the section, together with the change from axial to transverse paleoflows, suggest more pronounced erosion of the frontal North Penninic and Ultrahelvetic nappes (Matter, 1964).

DISCUSSION

The structure, stratigraphy, and petrography of the Molasse strata presented previously herein record the development of the Alpine thrust wedge–Molasse basin system through time. In the following sections, the causal relationships between the major orogenic events on the initiation and duration of each dispersal system are discussed. Subsequently, the evolution of the geometric shape and facies architecture of the basin is reconstructed in relation to thrust-wedge evolution and processes, such as in-sequence and out-of-sequence thrusting, backthrusting, and underplating.

Relationships Between Alpine Evolution and Dispersal System Activity

The present-day Alpine hinterland of the study area consists of the following structural units: the Helvetic zone, which is subdivided in a lower Infrahelvetic complex (Aar massif and its autochthonous-parautochthonous cover) and an upper Helvetic (sensu stricto) complex (Helvetic thrust nappes), separated by the basal Alpine thrust. The Helvetic zone, in turn, is overlain by a piggyback stack of Penninic and Austroalpine nappes (Fig. 11).

Chronostratigraphic and petrographic data from the Molasse strata reveal erosion of the Austroalpine and Penninic nappes of eastern Switzerland during the entire Chattian and early Aquitanian—i.e., from 30 to 22 Ma (Rigi and Höhronen systems). First, conglomerates rich in carbonate clasts were deposited on the Rigi alluvial fan between about 30 and 25.5 Ma. This depositional episode coincides with the Insubric phase of backthrusting that has been interpreted to result in >10 km of vertical displacement (Hurford, 1986; Schmid et al., 1989). During the same time span (30–25 Ma), the intrusion of the Bergell (ca. 30 Ma) and Novate (ca. 26 Ma) plutons occurred (Gulson, 1973; Koeppel and Grünenfelder, 1975). Synmagmatic backthrusting along the Insubric Line is likely to have increased the denudation rates of the Penninic and Austroalpine nappes of eastern Switzerland. As a result, submarine boulder conglomerates were deposited in the Gonfolite Lombarda south of the Alps (Gunzenhauser, 1985), and construction of the Rigi fan began. However, the distance from the source area to the basin margin was much larger for the Rigi river than for the system feeding the Gonfolite Lombarda. This conclusion is based on studies on conglomerate provenance (Speck, 1953; Müller, 1971; Giger, 1991), which suggest a water divide between both catchment areas immediately north of the Bergell intrusion. After restoration to their prethrusting positions, the resulting distance between the source area and receiving basins is on the order of 40–50 km for the Gonfolite Lombarda and 70–80 km for the Rigi dispersal system. There are, however, indications that backthrusting of Austroalpine and Penninic units had already commenced by about 35–30 Ma (Mancktelow, 1990). This is reflected in the presence of Rupelian conglomerates in the Gonfolite Lombarda (Gunzenhauser, 1985). During that same time, turbidites gradually filled the submarine trough of the North Alpine foreland, forming the regressive sequence of the UMM (Diem, 1986).

The Aar massif also underwent major uplift in Miocene and Pliocene time (Kammer, 1989; Burkhard, 1990; Lihou et al., 1995; Pfiffner et al., 1996b). The massif was buried by stacking of Alpine nappes in the course of thrust wedge advance (Pfiffner et al., 1996b). Stacking of nappes resulted in an increase in temperature and pressure, reaching greenschist facies conditions of about 350 °C in the buried Aar massif (Niggli, 1970; Frey et al., 1980a, 1980b; Erdelbrock, 1994) by 25 Ma at the latest (Hunziker et al., 1986). Such metamorphic conditions correspond to a burial depth of at least 12 km, if we use an

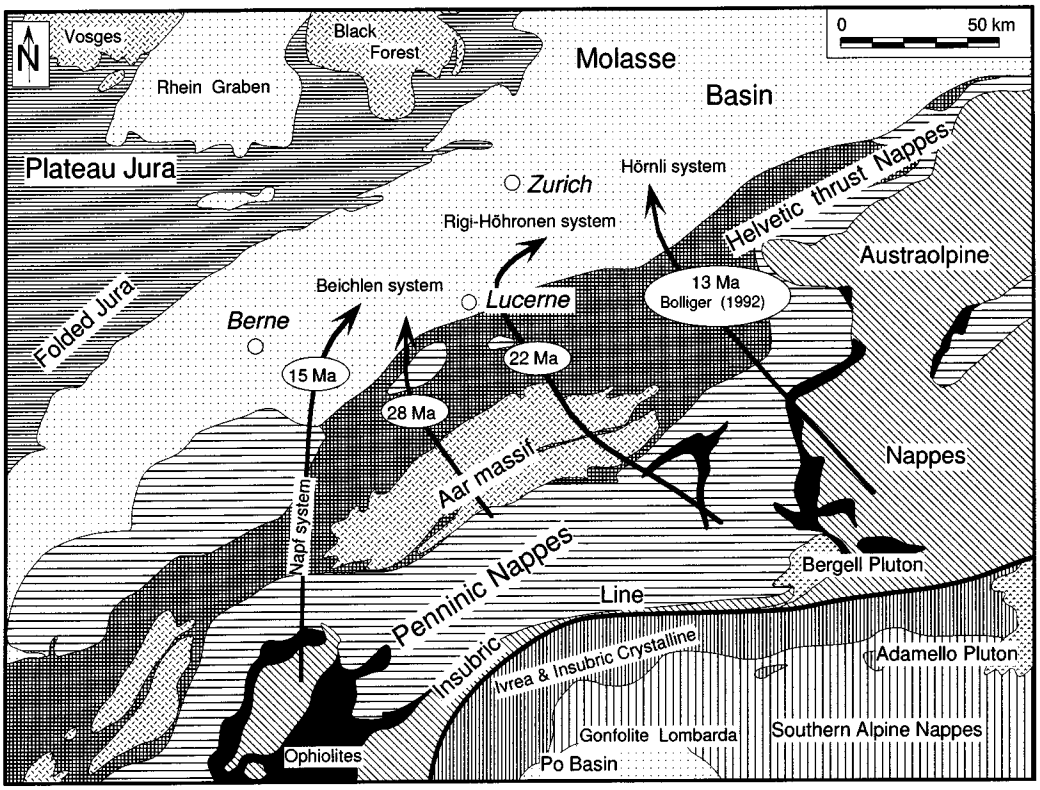

Figure 11. Tectonic map of the central Alps. Arrows represent the major dispersal systems in the central Swiss Molasse basin. Circled dates indicate cessation of drainage systems.

average geothermal gradient of 30 °C/km as postulated for the central Alps (Pfiffner, 1986; Hurfurd et al., 1991; Erdelbrock, 1994; Pfiffner et al., 1996b). Subsequent exhumation caused cooling through the "annealing temperature windows" of the apatite and zircon fission track systems. Zircon fission tracks chronicle cooling through the 200–250 °C temperature window, which corresponds to a burial depth of ≈8 km, whereas apatite fission tracks record cooling through the 80–120 °C temperature window, which is equivalent to a burial depth of about 4 km (Hurford et al., 1991). Cooling histories based on zircon and apatite fission-track data from the external massifs (Hurford, 1986; Soom, 1990; Michalski and Soom, 1990) suggest that the eastern Aar massif reached shallow crustal levels of ≈8 km at about 20 Ma. Thus, at this time, the piggyback stack of Penninic and Austroalpine nappes overlying the eastern Aar massif had apparently been denuded by at least 4 km due to uplift of the eastern Aar massif (Pfiffner et al., 1996b). The erosional products are now found in the Rigi and Höhronen fans. The fission-track data suggest that, in early Miocene time, the zone of maximum denudation and bedrock uplift shifted from the Insubric Line to the Aar massif, which was at least 40 km to the north (see also Sinclair and Allen, 1992). This northward shift would have significantly reduced the size of the catchment area of the early Miocene Höhronen river compared to that of the late Oligocene Rigi river. The drainage reconfiguration resulting from deformation of the Aar massif might thus explain the deactivation of the Höhronen dispersal system at approximately 22 Ma (Figs. 10 and 11). This interpretation is supported by the time of deactivation of the adjacent major dispersal systems (Fig. 11): The Napf and Hörnli drainage systems to the west and east of the Aar massif were active until about 15 and 13 Ma, respectively, whereas the Höhronen and Beichlen rivers, which had to cross the Aar massif, were deactivated much earlier (Schlunegger, 1995). One might expect that bedrock uplift of the Aar massif would lead to the establishment of new large dispersal systems in the foreland. This was not the case in the proximal Molasse, because deformation of the Aar massif was coupled with thrusting in the Molasse basin (Pfiffner et al., 1996a), which became, as discussed later herein, subject to erosion and redeposition on bajada fans at this time.

Tectonic Processes in the Alpine Orogen, Basin Geometry, and Facies Architecture

In early Chattian time, the Penninic and Austroalpine nappes had already been emplaced (Burkhard, 1988). These units overlay the Helvetic thrust nappes, which underwent low-grade metamorphism sometime between 30 and 35 Ma (Frey et al., 1973, 1980a; Groshong et al., 1984; Hunziker et al., 1992). Thrusting of the Helvetic thrust nappes above the Infrahelvetic complex (Aar massif and its autochthonous to parautochthonous cover) along the basal Alpine thrust resulted in low-grade metamorphism in the latter units between 20 and 25 Ma (Niggli, 1970; Frey et al., 1980b; Erdelbrock, 1994; Rahn et al., 1994, 1995). Thrusting of the Helvetic thrust nappes in eastern Switzerland (Calanda phase; Milnes and Pfiffner, 1977, 1980) seems to have been contemporaneous with the Insubric phase of backthrusting (Burkard, 1988), which started in southeastern Switzerland prior to 30 Ma and reached maximum uplift rates between 30 and 25 Ma (Hurford, 1986; Schmid et al., 1989). A subsequent forward thrusting event along the basal Alpine thrust was identified by a discontinuity in the metamorphic gradient between the Helvetic thrust nappes and the Infrahelvetic complex (Frey et al., 1980b; Frey, 1988), which resulted in an amount of post 20–25 Ma offset on the order of 5–10 km (Erdelbrock, 1994; Rahn et al., 1995; Wang et al., 1995). This tectonic event has been termed the "Ruchi phase of deformation" (Milnes and Pfiffner, 1977, 1980).

Another Alpine unit that underwent intense deformation during deposition of the Molasse strata is the Infrahelvetic complex. The exhumation history of this unit was reconstructed by using the temporal calibration of the "annealing closing

temperatures" of zircon and apatite fission-track systems (Michalski and Soom, 1990; Soom, 1990) and by using relationships between metamorphic fabrics and structures (Pfiffner, 1982; Groshong et al., 1984). These data suggest initial bedrock uplift and denudation of the eastern Aar massif and its cover in the early Miocene (ca. 23–20 Ma), which appears to represent the Calanda phase of deformation (Milnes and Pfiffner, 1977, 1980). This in turn is coupled with thrusting in the Subalpine Molasse (Pfiffner et al., 1996b). Final uplift of the Aar massif occurred in late Miocene–Pliocene time and is associated with folding and thrusting of the Jura Mountains (Lihou et al., 1995; Pfiffner et al., 1996a).

The structural evolution in the orogen, as discussed above, yields a relative sequence of deformation events with fairly well constrained numerical ages for each phase. In this section, we discuss the geometrical, sedimentological, petrographic, and structural evolution of the proximal Molasse of central Switzerland in three time slices in relation to tectonic events in the orogen.

The tectonostratigraphic configuration of the study area at 25.5 Ma (Fig. 12A) is based on measured thicknesses of USM I in the Hünenberg-1, Entlebuch-1, and Rigi sections, on determination of the petrofacies (Figs. 9, 10), and on the palinspastic restoration of the Subalpine Molasse shown in Figure 3C. This configuration shows that the Alpine front was formed mainly by North Penninic and Ultrahelvetic Flysch nappes, which were shedding their detritus northward to the bajada fans. The Helvetic thrust nappes, which form the present-day Alpine border, had to be buried under the stack of the tectonically higher Penninic nappes at that time (Matter, 1964; Stürm, 1973). At the thrust front, the Molasse basin formed a wedge-shaped trough >37 km wide that was filled in its proximal part with a 4-km-thick succession of predominantly conglomerates deposited by the prograding Rigi system (Rigi fan) and by local-source rivers on bajada fans. In order to determine the dip angle for the basement at the toe of the wedge, surface slopes and stratigraphic tapers must be considered. Although surface slopes of alluvial fans in foreland basins are poorly known, Jordan et al. (1988) argued that a total of 300–400 m stratal thickness is attributable to elevation change in prograding alluvial fan systems in a foreland basin. Using an additional 200 m for the UMM beneath the Rigi section (Greber et al., 1994) results in a dip angle of 6°–7° for the basement at the toe of the wedge (Fig. 12A). An enhanced flexure hypothesis at the proximal basin margin is supported by an increase in sediment accumulation rate from 0.7 to >1.0 km/m.y. in the Rigi section. Between Entlebuch-1 and Hünenberg-1, USM I is less than 500 m thick and is even slightly repeated by a thrust in Entlebuch-1 (Vollmayr and Wendt, 1987). In this part of the basin, predominantly mudstones and sandstones were deposited by an axial system derived from farther west at a rate of <0.3 km/m.y. The different petrofacies and sedimentary trends at Rigi, when compared to those at Hünenberg-1 and Entlebuch-1, suggest that progradation of the Rigi fan was restricted. This phase of basin evolution coincides with the Insubric phase of backthrusting along the Insubric Line approximately 100 km south of the Rigi fan and with a phase of forward thrusting along the basal Alpine thrust (Calanda phase). Subsidence driven by crustal loading in the central orogen appears to have restricted progradation of the Rigi fan, whereas the loading, in combination with forward thrusting, seems to have caused increased erosion and redeposition of frontal North Penninic and Ultrahelvetic Flysch units on bajada fans and to have created a wedge-shaped basin.

This first phase of basin formation is succeeded by a basinwide unconformity at about 25 Ma. No major loading and forward-thrusting events are recorded in the Alpine orogen for that time, according to cooling ages and metamorphic and radiometric studies (Hurford, 1986; Frey, 1988; Schmid et al., 1989). It appears that this phase of tectonic quiescence was responsible for uplift and erosion across the whole basin at 25 Ma (see also Flemings and Jordan, 1990).

The second phase of basin fill history spans the time interval between ca. 24 and 23 Ma. Reconstruction of the basin geometry for that time interval is difficult because we do not see the base of USM II at Höhronen (Schlanke, 1974) and because time control in the Hünenberg-1 section is rather speculative. Nonetheless it seems that during an initial stage the more distal sites located at Hünenberg-1 subsided more rapidly than the more proximal ones, represented by the Höhronen section (Fig. 8). Furthermore, no 25–23-m.y.-old sediments are present in the most proximal basin at Rigi, suggesting bypassing or erosion. This phase of basin evolution is interpreted as the flexural response of the basin to renewed initial loading in the orogen after a phase of tectonic quiescence. This bypassing may result from initiation of motion on the Rigi thrust and initial uplift and erosion of the most proximal part of the foreland.

The cross section representing the foreland basin-thrust-wedge configuration at 21.5 Ma (Fig. 12B) is based on lithofacies, thicknesses, and magnetostratigraphies of measured sections, the palinspastic restoration of the Subalpine Molasse shown in Figure 3C, and the strong diminution of North Penninic and Ultrahelvetic Flysch clasts in comparison with USM I. As for the reconstruction of the 25 Ma basin architecture, a total of 300–400 m of stratigraphic thickness is attributed to elevation (Jordan et al., 1988). The cross section shows a flexural angle of 5° for the underlying basement and a wedge-shaped basin filled by conglomerates and mudstones south of the Fischenbach section, which were deposited by the Höhronen system and local-source rivers. In the more distal part of the foreland, however, no conglomerates were deposited, and a monotonous series of mudstones and sandstones predominates. The latter unit was deposited by the axial Napf dispersal system (Figs. 9, 10). As with the Rigi fan, the northward progradation of the Höhronen was probably controlled by the relatively rapid subsidence of the proximal basin in comparison to the sediment supply. During this interval, proximal parts of the USM I were incorporated into the orogenic wedge by in-sequence thrusting, as evidenced by redeposited Rigi fan conglomerates on bajada fans (unit C of the Höhronen section). The recycling of the Rigi conglomerates into the Höhronen fan contrasts with previous interpretations of the origin of this unit, which represented it either as a transition from Rigi to Höhronen dispersal system (Schlanke, 1974) or as a mixture of both Alpine rivers (Müller, 1971). The end of this phase is marked by an unconformity within USM II (see Fig. 7), which spans the studied part of the basin.

The dip of the basement under the proximal foreland appears to be slightly shallower (Fig. 12B) than in the previous reconstruction (25.5 Ma; Fig. 12B). Thrusting and incorporation of USM I into the orogenic wedge coincides with the Calanda phase of deformation in the Infrahelvetic complex between ca. 23 and 20 Ma. According to Pfiffner et al. (1996b) this phase of deformation caused initial bedrock uplift of the Aar massif by about 4 km and forward propagation of the orogenic wedge. Loading in the northern part of the central orogen and forward thrusting seem to be the major controls on the basin geometry and architecture during this time period. However, crustal loading of the Infrahelvetic complex is probably small compared to the effect of >10 km of vertical displacement, which occurred in southeastern Switzerland during the Insubric phase of backthrusting. These differences might explain the slight reduction of the flexural angle of the underlying basement at the end of this phase. Part of the decreased dip might result also from rebound that occurred during the preceding quiescence. In addition, by 21 Ma, the proximal USM I was incorporated into the orogenic wedge. This represents an event of accretion at the toe of the wedge, as opposed to stable sliding of the entire wedge. Accretion simply redefined the leading edge of the wedge as being farther on to the flexed plate. Given the likelihood of rapid erosion of the uplifted USM I (see also Burbank and Beck, 1991), no significant new loads would have been added above the flexed plate by this

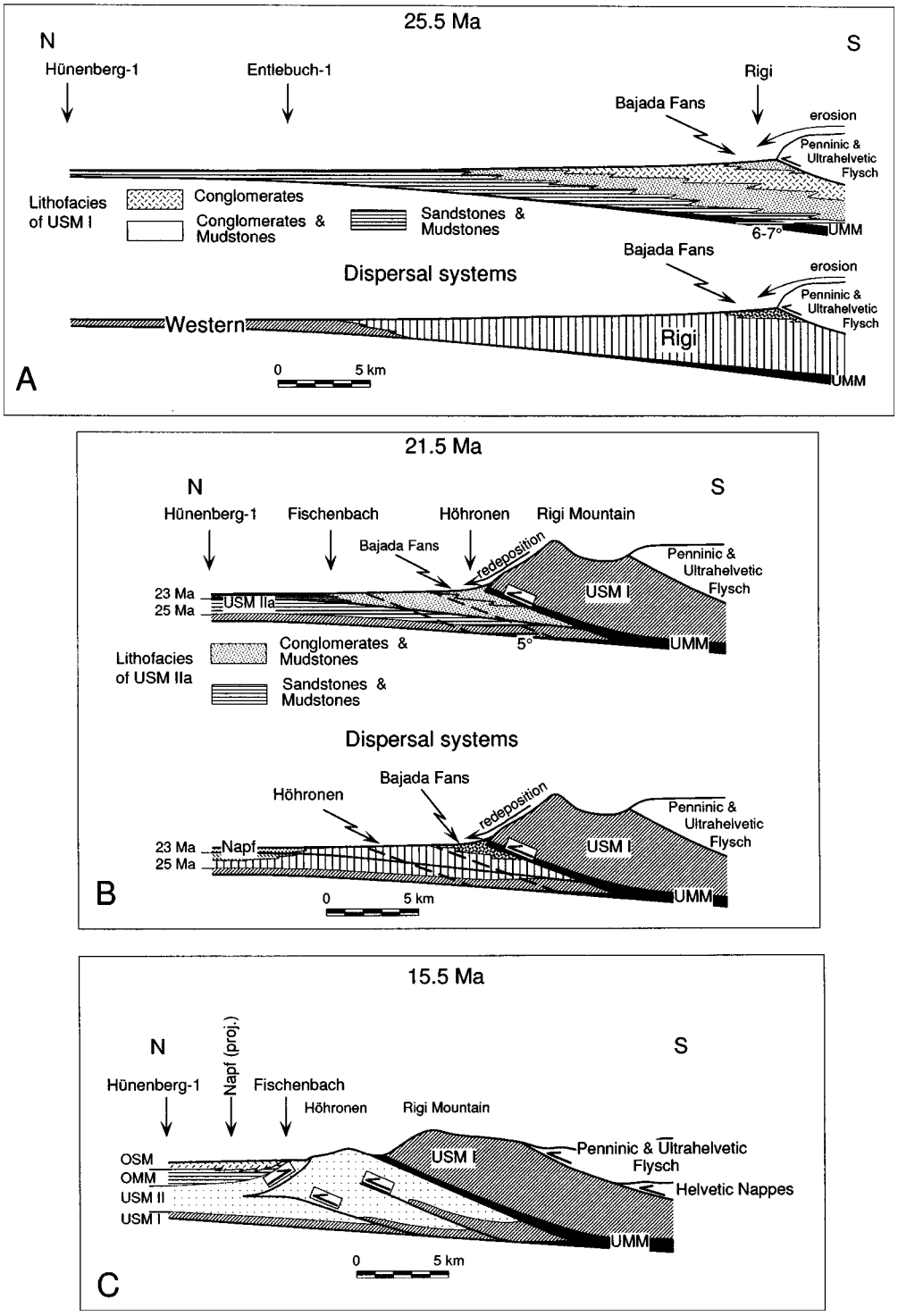

Figure 12. (A) Schematic diagram showing the tectonostratigraphic configuration of the Molasse basin at 25.5 Ma. A wedge-shaped basin was created as a result of crustal loading by the Insubric phase of backthrusting along the Insubric Line and by forward thrusting of North Penninic and Ultrahelvetic Flysch nappes onto the Alpine foreland. Forward thrusting at the tip of the orogenic wedge resulted in uplift, erosion, and redeposition of the frontal Alpine units on bajada fans. (B) Sketch illustrating the stratigraphy and structure of the basin margin at 21.5 Ma. It shows incorporation of proximal USM I into the thrust wedge and redeposition of conglomerates derived from the Rigi fan on bajada fans. Uplift of the Rigi thrust sheet and loading by underplating of the Aar massif resulted in renewed flexural subsidence of the Molasse. (C) Reconstruction of the tectonostratigraphic configuration of the proximal basin margin at 15.5 Ma, revealing that underplating of Molasse deposits resulted in backthrusting at the southern margin of the Plateau Molasse and in formation of a south-vergent progressive unconformity.

accretion. Thus, the shape of the flexural depression would not change, but the proximal edge of the depositional foreland would be shifted northward above more gently flexed crust.

Farther northward, propagation of the thrust system into the Höhronen (Fig. 12B, dashed lines) would have caused rock uplift in the hanging walls. Denudation in response to this deformation is a likely cause of the unconformity at 21.5 Ma (Fig. 7).

The reconstruction of the tectonostratigraphic configuration at 15.5 Ma (Fig. 12C) depicts the penultimate major deformation and related deposition in the study area. It shows in-sequence incorporation of USM II and OMM into the orogenic wedge and development of the backthrust and Triangle Zone. This interpretation is supported by (1) a gradually decreasing accumulation rate from 0.5 to 0.35 km/m.y. adjacent to the backthrust, (2) southward onlap of OSM on OMM, and (3) the south-vergent progressive unconformity in the OSM north of the backthrust. The origin of the basal Burdigalian unconformity at 20 Ma might be caused by forward propaga-

tion of the thrust front into the more distal part of the basin. The discordance at 18 Ma, however, is related to a sea-level drop proposed by Keller (1989) in the upper part of the OMM and also represented on seismic lines as a major sequence boundary (Schlunegger et al., in press). Finally, the decreasing accumulation rates during progradation of the Napf fan, as recorded by the coarsening- and thickening-upward megasequence in the Napf section, suggest that fan progradation was caused by a relative drop in subsidence.

The final stage of basin evolution, from 15.5 to 15 Ma, is characterized by thrusting of the Helvetic nappes and the piggyback stacking of North Penninic and Ultrahelvetic nappes along the basal Alpine thrust. This interpretation is based on (1) increasing accumulation rates up-section in the Napf fan from 0.35 to >1.0 km/m.y., suggesting additional loading; (2) an angular unconformity between the conglomerates of the Rigi thrust sheet and the basal Alpine thrust, indicating that thrusting of the Helvetic border chain postdates uplift of the Rigi thrust sheet (out-of-sequence thrusting); (3) an increasing admixture and size of North Penninic and Ultrahelvetic Flysch clasts associated with a change from predominantly axial to transverse drainage, implying increased erosion of the frontal Alpine nappes; and (4) first appearance of Helvetic clasts in the OSM farther east (Leupold et al., 1942; Tanner, 1944). Out-of-sequence forward thrusting in the Helvetic nappes along the basal Alpine thrust at ca. 15 Ma is interpreted to represent the Ruchi phase of deformation (Milnes and Pfiffner, 1978, 1980), which caused a horizontal displacement of ≈5–10 km (Erdelbrock, 1994; Rahn et al., 1995; Wang et al., 1995). This interpretation, however, is in disagreement with Schmid et al. (1996), who suggested that this phase of deformation occurred in early Miocene time. It is not yet certain whether increased accumulation of conglomerates in the Napf fan was additionally enhanced by increased bedrock uplift in the Aar massif at that time.

CONCLUSIONS

Detailed chronologic, petrographic, sedimentological and structural analysis of the proximal Molasse strata of central Switzerland provides for the first time a precise calibration of the depositional processes and the geometrical evolution of the basin. Petrofacies and large-scale coarsening- and thickening-upward megasequences, which have been traditionally distinguished in the Molasse, are related to the uplift history of the central Alps and to tectonic processes such as in-sequence and out-of-sequence thrusting as well as to underplating at the tip of the orogenic wedge.

Determination of petrofacies in the detailed temporal framework allows reconstruction of the denudation history of the Alpine hinterland in relation to its exhumation. The Insubric phase of backthrusting, which occurred in southeastern Switzerland between 30 and 25 Ma, resulted in increased erosion of the Austroalpine and Penninic nappes of eastern Switzerland and in activation of the Rigi dispersal system. Downcutting of these nappes to their crystalline cores is recorded in the Molasse strata by an increase in crystalline clasts in the conglomerates. Subsequent initial uplift of the Aar massif 40 km farther north delineated the time span during which dispersal systems were active. The Höhronen dispersal system, which crossed the Aar massif on its eastern flank, was deactivated at 22 Ma, whereas the Napf and the Hörnli drainage systems to the west and east of the Aar massif were active until about 15 and 13 Ma, respectively, which indicates that they were not affected by the initial uplift.

The detritus shed from the evolving Alpine orogen was deposited in a foreland basin whose geometry changed according to thrusting events in the orogen. During phases of uplift in the central orogen and forward thrusting at the tip of the orogenic wedge, a wedge-shaped basin formed, characterized by a high lateral gradient, the accumulation rate ranging from more than 1 km/m.y. adjacent to the tip of the orogenic wedge to only 0.3 km/m.y. in the more distal settings. Conglomerates deposited in river channels, on alluvial fans, and on bajada fans are the characteristic lithofacies in proximal reaches of this basin type, whereas channel sandstone bodies embedded in overbank fines are found in axial river systems in more distal positions. A change in the load in the Alpine orogen by tectonic quiescence after a major loading event or by activation of a new thrust in the proximal foreland caused major unconformities in the study area.

High-resolution reconstruction of the structural and geometrical evolution of the proximal Molasse strata reveals in-sequence and out-of-sequence thrusting events at the Alpine front and incorporation of the Molasse into the orogenic wedge by in-sequence thrusting and underplating. Furthermore, it reveals close relationships between periods of rapid denudation in the central Alps and phases of increased sediment accumulation rates at the proximal basin border. An initial increase in Molasse accumulation rates to >1 km/m.y. associated with the development of a large-scale coarsening- and thickening-upward megasequence occurred between 30 and 25.5 Ma and coincides with the Insubric phase of backthrusting along the eastern Insubric Line and forward propagation of the Alpine wedge along the basal Alpine thrust. The end of this tectonic event is marked by a basinwide unconformity, interpreted to result from crustal rebound after initial loading. A subsequent increase in accumulation rates to >1 km/m.y. between 23 and 21.5 Ma coincides with initial uplift of the eastern Aar massif and with incorporation of early Chattian conglomerates into the orogenic wedge. The third advance of the Alpine wedge between 21 and 15.5 Ma caused underplating of Molasse deposits, resulting in synsedimentary backthrusting of previously deposited Molasse sequences and in the development of a progressive unconformity. A third increase in accumulation rates to >1 km/m.y. between 15.5 and 15 Ma marks the final loading event in the wedge, an event coeval with out-of-sequence thrusting of the Helvetic border chain and of the piggyback stack of North Penninic and Ultrahelvetic Flysch nappes along the basal Alpine thrust.

ACKNOWLEDGMENTS

This project was carried out as part of Schlunegger's Ph.D. project, with funding provided by the Swiss National Science Foundation (grant 21-36219.91). We thank B. Engesser and C. Mödden, who identified the mammal fragments; S. Lund, who advised us in interpreting the demagnetization data; H. Haas, for the time-consuming heavy-mineral separation; M. Mange, for determination of heavy minerals; H. Bärtschi, for technical instructions; S. Henyey, for processing numerous magnetic samples; S. Burns, for help with English; A. Pfiffner, G. Schreurs, O. Kempf, and P. Strunck for fruitful discussions; and Schlunegger's colleagues, who acted as assistants and climbing instructors. Constructive reviews by C. Paola and D. McNeill greatly improved the quality of the manuscript.

REFERENCES CITED

Beaumont, C., 1981, The evolution of sedimentary basins on a viscoelastic lithosphere: Theory and examples: Geophysical Journal of the Royal Astronomical Society, v. 65, p. 291–329.

Berli, S., 1985, Die Geologie des Sommersberges (Kantone St. Gallen und Appenzell): Berichte der St. Gallischen naturforschenden Gesellschaft, v. 82, p. 112–145.

Burbank, D. W., Raynolds, R. G. H., and Johnson G. D., 1986, Late Cenozoic tectonics and sedimentation in the northwestern Himalayan foredeep: II. Eastern limb of the northwest syntaxis and regional synthesis, *in* Allen, P. A., and Homewood, P., eds., Foreland basins: International Association of Sedimentologists Special Publication 8, p. 293–306.

Burbank, D. W., and Beck R. A., 1991, Rapid, long-term rates of denudation: Geology, v. 19, p. 1169–1172.

Burbank, D. W., Engesser, B., Matter, A., and Weidmann M., 1992, Magnetostratigraphic chronology, mammalian faunas, and stratigraphic evolution of the Lower Freshwater Molasse, Haute-Savoie, France: Eclogae Geologicae Helvetiae, v. 85, p. 399–431.

Burkhard, M., 1988, L'Hélvetique de la bordure occidentale du massif de l'Aar (évolution tectonique et métamorphique): Eclogae Geologicae Helvetiae, v. 81, p. 63–114.

Burkhard, M., 1990, Aspects of the large-scale Miocene deformation in the most external part of the Swiss Alps (Subalpine Molasse to Jura fold belt): Eclogae Geologicae Helvetiae, v. 83, p. 559–583.

Buxtorf, A., Tobler, A., Niethammer, G., Baumberger, E., Arbenz, P., and Staub, W., 1916, Geologische Vierwaldstättersee-Karte: Schweizerische Geologische Kommission Spezialkarte Nr. 66a, scale 1:50 000.

Cande, S. C., and Kent D. V., 1992, A new geomagnetic polarity time-

scale for the Late Cretaceous and Cenozoic: Journal of Geophysical Research, v. 97, p. 13917–13951.
Cande, S. C., and Kent D. V., 1995, Revised calibration of the geomagnetic polarity timescale for the Late Cretaceous and Cenozoic: Journal of Geophysical Research, v. 100, p. 6093–6095.
Colombo, F., 1994, Normal and reverse unroofing sequences in syntectonic conglomerates as evidence of progressive basinward deformation: Geology, v. 22, p. 235–238.
Colombo, F., and Vergés, J., 1992, Geometria del margen S.E. de la Cuenca del Ebro: Discordancias progresivas en el Grupo Scala Dei, Serra de La Llena (Tarragona): Acta Geologica Hispania, v. 27, p. 33–53.
Diem, B., 1986, Die Untere Meeresmolasse zwischen der Saane (Westschweiz) und der Ammer (Oberbayern): Eclogae Geologicae Helvetiae, v. 79, p. 493–559.
Engesser, B., 1990, Die Eomyidae (Rodentia, Mammalia) der Molasse der Schweiz und Savoyens. Systematik und Biostratigraphie: Schweizerische Paläontologische Abhandlungen, v. 112, 144 p.
Erdelbrock, K., 1994, Diagenese und schwache Metamorphose im Helvetikum der Ostschweiz 'Inkohlung und Illit-"Kristallinität" [Ph.D. dissert.]: Aachen, Germany, University of Aachen, 220 p.
Fisher, R. A., 1953, Dispersion on a sphere: Proceedings of the Royal Society of London, ser. A, v. 217, p. 295–305.
Flemings, P. B., and Jordan, T. E., 1990, Stratigraphic modeling of foreland basins: Interpreting thrust deformation and lithospheric rheology: Geology, v. 18, p. 430–434.
Frey, M., 1988, Discontinuous inverse metamorphic zonation, Glarus Alps, Switzerland: Evidence from illit "crystallinity" data: Schweizerische Mineralogische und Petrogragraphische Mitteilungen, v. 68, p. 171–183.
Frey, M., Hunziker, J. C., Roggwiller, P., and Schindler, C., 1973, Progressive niedriggradige Metamorphose glaukonitführender Horizonte in den helvetischen Alpen der Ostschweiz: Contributions to Mineralogy and Petrology, v. 39, p. 185–218.
Frey, M., Bucher, K., Frank, E., and Mullis, M., 1980a, Alpine metamorphism along the Geotraverse Basel-Chaisso—A review: Eclogae Geologicae Helvetiae, v. 73, p. 527–546.
Frey, M., Teichmüller, M., Teichmüller, R., Mullis, J., Künzi, B., Breitschmid, A., Grunder, U., and Schwizer, B., 1980b, Very low-grade metamorphism in the external parts of the Central Alps: Illite crystallinity, coal rank and fluid inclusion data: Eclogae Geologicae Helvetiae, v. 73, p. 173–203.
Füchtbauer, H., 1959, Die Schüttungen im Chatt und Aquitan der deutschen Apenvorlandmolasse: Eclogae Geologicae Helvetiae, v. 51, p. 928–941.
Füchtbauer, H., 1964, Sedimentpetrographische Untersuchungen in der älteren Molasse nördlich der Alpen: Eclogae Geologicae Helvetiae, v. 61, p. 157–298.
Gasser, U., 1966, Sedimentologische Untersuchungen in der äusseren Zone der subalpinen Molasse des Entlebuchs (Kt. Luzern): Eclogae Geologicae Helvetiae, v. 59, p. 723–772.
Gasser, U., 1967, Erste Resultate über die Verteilung von Schwermineralen in verschiedenen Flyschkomplexen der Schweiz: Geologische Rundschau, v. 56, p. 300–308.
Gasser, U., 1968, Die innere Zone der subalpinen Molasse des Entlebuchs (Kt. Luzern), Geologie und Sedimentologie: Eclogae Geologicae Helvetiae, v. 61, p. 229–313.
Giger, M., 1991, Geochronologische und petrographische Studien an Geröllen und Sedimenten der Gonfolite Lambarda Gruppe (Südschweiz und Norditalien) und ihr Vergleich mit dem alpinen Hinterland [Ph.D. dissert.]: Bern, Switzerland, University of Bern, 227 p.
Greber, E., Günenfelder, T., Keller, B., and Wyss, R., 1994, Die Geothermie-Bohrung Weggis, Kanton Luzern: Bulletin der Vereinigung Schweizerischer Petroleum-Geologen und -Ingenieure, v. 61, p. 17–43.
Groshong, R. H., Jr., Pfiffner, O. A., and Pringle, L. R., 1984, Strain partitioning in the Helvetic thrust belt of Eastern Switzerland and from the leading edge to the external zone: Journal of Structural Geology, v. 6, p. 5–18.
Gulson, B. L., 1973, Age relations in the Bergell region of the southeast Swiss Alps, with some geochemical comparisons: Eclogae Geologicae Helvetiae, v. 66, p. 293–314.
Gunzenhauser, B. A., 1985, Zur Sedimentologie und Paläogeographie der oligo-miocaenen Gonfolite Lombarda zwischen Lago Maggiore und der Brianza (Südtessin, Lombardei): Schweizerische Geologische Kommission, Beiträge zur geologischen Karte der Schweiz, NF 159, 95 p.
Haldemann, E. G., Haus, H. A., Holliger, A., Liechti, W., Rutsch, R. F., and Della Valle, G., 1980, Geologischer Atlas der Schweiz, Blatt 1188 Eggiwil (Nr. 75): Schweizerische Geologische Kommission, scale 1:25 000, 1 sheet.
Haus, H., 1937, Geologie der Gegend von Schangnau im oberen Emmental (Kt. Bern). Ein Beitrag zur Stratigraphie und Tektonik der subalpinen Molasse und des Alpenrandes: Schweizerische Geologische Kommission, Beiträge zur geologischen Karte der Schweiz, NF 75, 93 P.
Homewood, P., Allen, P. A., and Williams, G. D., 1986, Dynamics of the Molasse basin of western Switzerland, *in* Allen, P. A., and Homewood, P., eds., Foreland basins: International Association of Sedimentologists Special Publication 8., p. 199–217.
Hunziker, J. C., Frey, M., Clauer, N., Dallmeyer, R. D., Friedrichsen, H., Flehmig, W., Hochstrasser, K., Roggwiller, P., and Schwander, H., 1986, The evolution of illite to muscovite: Mineralogical and isotopic data from the Glarus Alps, Switzerland: Contributions to Mineralogy and Petrology, v. 92, p. 157–180.
Hunziker, J. C., Desmons, J., and Hurford, A. J., 1992, Thirty-two years of geochronological work in the Central and Western Alps: A review on seven maps: Mémoires de Géologie (Lausanne), v. 13, 59 p.
Hurford, A. J., 1986, Cooling and uplift patterns in the Lepontine Alps, south central Switzerland and an age of vertical movement on the Insubric fault line: Contributions to Mineralogy and Petrology, v. 93, p. 413–427.
Hurford, A. J., Hunziker, J. C., and Stöckert, B., 1991, Constraints on the late thermotectonic evolution of the Western Alps: Evidence for episodic rapid uplift: Tectonics, v. 10, p. 758–769.
Hurni, A., 1991, Geologie und Hydrogeologie des Truebtales [Master's thesis]: Bern, Switzerland, University of Bern, 153 p.
Jordan, T. E., 1981, Thrust loads and foreland basin evolution, Cretaceous, western United States: American Association of Petroleum Geologists Bulletin, v. 65, p. 2506–2520.
Jordan, T. E., Flemings, P. B., and Beer, J. A., 1988, Dating thrust-fault activity by use of foreland-basin strata, *in* Kleinspehn, K. L., and Paola, C., eds., New perspectives in basin analysis: New York, Springer-Verlag, p. 307–330.
Kammer, A., 1989, Alpidische Verformung des aarmassivischen Nordrandes: Schweizerische Mineralogische und Petrographische Mitteilungen, v. 69, p. 37–53.
Keller, B., 1989, Fazies und Stratigraphie der Oberen Meeresmolasse (Unteres Miozän) zwischen Napf und Bodensee [Ph.D. dissert.]: Bern, Switzerland, University of Bern, 277 P.
Keller, B., Bläsi, H.-R., Platt, N. H., Mozley, P. S., and Matter, A., 1990, Sedimentäre Architektur der distalen Unteren Süsswassermolasse und ihre Beziehung zur Diagenese und den petrophysikalischen Eigenschaften am Beispiel der Bohrungen Langenthal: Geologische Berichte No. 13, Landeshydrologie und -geologie, 100 p.
Kleiber, K., 1937, Geologische Untersuchungen im Gebiet der Hohen Rone: Eclogae Geologicae Helvetiae, v. 30, p. 419–430.
Koeppel, V., and Grünenfelder, M., 1975, Concordant U-Pb ages of monazite and xenotime from the Central Alps and the high-temperature Alpine metamorphism, a preliminary report: Schweizerische Mineralogische und Petrographische Mitteilungen, v. 55, p. 129–132.
Kopp, J., Bendel, L., and Buxtorf, A., 1955, Geologischer Atlas der Schweiz, Blatt 1150, Luzern (Nr. 28): Schweizerische Geologische Kommission, scale 1:25 000, 1 sheet.
Lemcke, K., Büchi, U. P., and Wiener, G., 1968, Einige Ergebnisse der Erdölexploration auf die mittelländische Molasse der Zentralschweiz: Bulletin der Vereinigung Schweizerischer Petroleum-Geologen und -Ingenieure, v. 35, p. 15–34.
Leupold, W., Tanner, H., and Speck, J., 1942, Neue Geröllstudien in der Molasse: Eclogae Geologicae Helvetiae, v. 33, p. 247–291.
Lihou J., Hurford, A., and Carter, A., 1995, Preliminary fission-track ages on zircons and apatites from the Sardona unit, Glarus Alps, eastern Switzerland: Late Miocene–Pliocene exhumation rates: Schweizerische Mineralogische und Petrographische Mitteilungen, v. 75, p. 177–186.
Mancktelow, N. S., 1990, The Simplon Fault Zone: Schweizerische Geologische Kommission, Beiträge zur geologischen Karte der Schweiz, NF 163, 74 p.
Matter, A., 1964, Sedimentologische Untersuchungen im östlichen Napfgebiet (Entlebuch—Tal der Grossen Fontanne, Kt. Luzern): Eclogae Geologicae Helvetiae, v. 57, p. 315–428.
Matter, A., Homewood, P., Caron, C., Rigassi, D., Van Stujivenberg, J., Weidmann, M., and Winkler, W., 1980, Flysch and molasse of western and central Switzerland, *in* Trümpy, R., ed., Geology of Switzerland, a guidebook, (Part B Excursions): Birkhäuser, Basel, Schweizerische Geologische Kommission, p. 261–293.
Matter, A., Peters, T., Bläsi, H.-R., Schenker, F., and Weiss, H.-P., 1988a, Sondierbohrung Schafisheim, Geologie, Beilagenband: Geologische Berichte No. 8, Landeshydrologie und -geologie, 89 sheets.
Matter, A., Peters, T., Bläsi, H.-R., Meyer, J., Ischi, H., and Meyer, Ch., 1988b, Sondierbohrung Weiach, Geologie, Textband: Geologische Berichte No. 6, Landeshydrologie und -geologie, 438 p.
Michalski, I., and Soom, M., 1990, The Alpine thermo-tectonic evolution of the Aar and Gotthard massifs, central Switzerland: Fission track ages on zircon and apatite and K-Ar mica ages: Schweizerische Mineralogische und Petrographische Mitteilungen, v. 70, p. 373–387.
Milnes, A. G., and Pfiffner, O. A., 1977, Structural development of the Infrahelvetic Complex, eastern Switzerland: Eclogae Geologicae Helvetiae, v. 70, p. 83–95.
Milnes, A. G., and Pfiffner, O. A., 1980, Tectonic evolution of the central Alps in the cross section St. Gallen–Como: Eclogae Geologicae Helvetiae, v. 73, p. 619–633.
Mödden, C., and Gad, J., 1992, Archaeomys-Arten (Theridomorpha, Rodentia) des oberoligozänen statigraphischen Referenz-Niveaus Boningen (Schweiz): Eclogae Geologicae Helvetiae, v. 86, p. 947–960.
Mödden, C., 1993, Revision der Archenomyimi Schlosser (Rodentia, Mammalia) des europäischen Oberoligozän: Schweizerische Pälontologische Anhandlungen, v. 115, 83 p.
Müller, H. P., 1971, Geologische Untersuchungen in der subalpinen Molasse zwischen Einsiedeln und oberem Zürichsee (Kt. Schwyz): Vierteljahresschrift der Naturforschenden Gesellschaft Zürich, v. 16, 153 p.
Niggli, E., 1970, Alpine Metamorphose und Alpine Gebirgsbildung: Fortschritte der Mineralogie, v. 47, p. 16–26.
Ottiger, R., Freimoser, M., Jäckli, H., Kopp, J., and Müller, E., 1990, Geologischer Atlas der Schweiz, Blatt 1131 Zug (Nr. 89): Schweizerische Geologische Kommission, scale 1:25 000.
Pfiffner, O. A., 1982, Deformation mechanisms and flow regimes in limestones from the Helvetic zone of the Swiss Alps: Journal of Structural Geology, v. 4, p. 429–442.
Pfiffner, O. A., 1986, Evolution of the north Alpine foreland basin in the central Alps, *in* Allen, P. A., and Homewood, P., eds., Foreland basins: International Association of Sedimentologists Special Publication 8, p. 219–228.
Pfiffner, O. A., Erard, P. F., and Stäuble, M., 1996a, Two cross sections through the Swiss Molasse basin, *in* Pfiffner, O. A., Lehner, P., Heitzmann, P., Müller, St., and Steck, A., eds., Deep structure of the Swiss Alps: Results of the National Research Program 20 (NRP 20): Birkhäuser, Basel, Schweizerische Geologische Kommission, p. 64–72.
Pfiffner, O. A., Sahli, S., and Stäuble, M., 1996b, Structure and evolution of the external basement massifs (Aar, Aiguilles Rouges/Mt. Blanc), *in* Pfiffner, O. A., Lehner, P., Heitzmann, P., Müller, St., and Steck, A., eds., Deep structure of the Swiss Alps: Results of the National Research Program 20 (NRP 20): Birkhäuser, Basel, Schweizerische Geologische Kommission, p. 139–153.
Rahn, M., Mullis, J., Erdelbrock, K., and Frey, M., 1994, Very low-grade metamorphism of the Taveyanne greywacke, Glarus Alps, Switzerland: Journal of Metamorphic Geology, v. 12, p. 625–641.
Rahn, M., Mullis, J., Erdelbrock, K., and Frey, M., 1995, Alpine metamorphism in the North Helvetic Flysch of the Glarus Alps, Switzerland: Eclogae Geologicae Helvetiae, v. 88, p. 625–178.
Renz, H. H., 1937, Die subalpine Molasse zwischen Aare und Rhein: Eclogae Geologicae Helvetiae, v. 30, p. 87–214.
Scherer, F., 1966, Geologisch-paläontologische Untersuchungen im Flysch und in der Molasse zwischen Thunersee und Eriz (Kt. Bern): Schweizerische Geologische Kommission, Beiträge zur geologischen Karte der Schweiz, NF 127, 115 p.
Schlanke, S., 1974, Geologie der subalpinen Molasse zwischen Biberbrugg/SZ, Hütten/ZH und Aegerisee/ZG, Schweiz: Eclogae Geologicae Helvetiae, v. 67, p. 243–331.
Schlunegger, F., 1995, Magnetostratigraphie und fazielle Entwicklung der Unteren Süsswassermolasse zwischen Aare und Limmat [Ph.D. dissert.]: Bern, Switzerland, University of Bern, 185 p.
Schlunegger, F., Matter, A., and Mange, M. A., 1993, Alluvial fan sedimentation and structure of the southern Molasse basin margin, Lake Thun area, Switzerland: Eclogae Geologicae Helvetiae, v. 86, p. 717–750.
Schlunegger, F., Burbank, D. W., Matter, A., Engesser, B., and Mödden, C., 1996, Magnetostratigraphic calibration of the Oligocene to middle Miocene (30–15 Ma) mammal biozones and depositional sequences of the Swiss Molasse basin: Eclogae Geologicae Helvetiae, v. 89, p. 753–788..
Schlunegger, F., Leu, W., and Matter, A., in press, Sedimentary sequences, seismofacies and stratigraphic simulation of the evolution of the Burdigalian/Langhian Upper Marine Molasse Group (OMM) of central Switzerland: American Association of Petroleum Geologists Bulletin.
Schmid, S. M., Aebli, H. R., Heller, F., and Zingg, A., 1989, The role of the Periadriatic Line in the tectonic evolution of the Alps, *in* Coward, M., Dietrich, D., and Park, R. G., eds., Alpine tectonics: Geological Society of London Special Publication 45, p. 153–171.
Schmid, S. M., Pfiffner, O. A., Schönborn, G., Froitzheim, N., and Kissling, E., 1996, Integrated cross section and tectonic evolution of the Alps along the eastern traverse, *in* Pfiffner, O. A., Lehner, P., Heitzmann, P., Müller, St., and Steck, A., eds., Deep structure of the Swiss Alps: Birkhäuser, Basel, Schweizerische Geologische Kommission, Results of the National Research Program 20 (NRP 20), p. 285–302.
Sinclair, H. P., and Allen, P. A., 1992, Vertical versus horizontal motions in the Alpine orogenic wedge: Stratigraphic response in the foreland basin: Basin Research, v. 4, p. 215–232.
Sinclair, H. D., Coakley, B. J., Allen P. A., and Watts, A. B., 1991, Simulation of foreland basin stratigraphy using a diffusion model of mountain belt uplift and erosion: An example from the central Alps, Switzerland: Tectonics, v. 10, p. 599–620.
Soom, M., 1990, Spaltspurdatierungen entlang des NFP 20-Westprofils (Externmassive und Penninikum): Schweizerische Mineralogische und Petrographische Mitteilungen, v. 69, p. 191–192.
Speck, J., 1953, Geröllstudien in der subalpinen Molasse am Zugersee und Versuch einer paläogeographischen Auswertung [Ph.D. dissert.]: Zürich, Switzerland, Universität Zürich, Kalt-Zahnder, Zug, 175 p.
Stürm, B., 1973, Die Rigischüttung. Sedimentpetrographie, Sedimentologie, Paläogeographie, Tektonik [Ph.D. dissert.]: Zürich, Switzerland, Universität Zürich, 98 p.
Tanner, H., 1944, Beitrag zur Geologie der Molasse zwischen Ricken und Hörnli: Mitteilungen des Geologischen Instituts ETH und Universität Zürich, v. C/22, 108 p.
Vollmayr, T., and Wendt, A., 1987, Die Erdgasbohrung Entlebuch-1, ein Tiefenaufschluss am Alpennordrand: Bulletin der Vereinigung Schweizerischer Petroleum-Geologen und -Ingenieure, v. 53, p. 67–79.
Wang, H., Frey, M., and Stern, W. B., 1995, Diagenesis and incipient metamorphism of the Helvetic Alps, eastern Switzerland: Clay mineral data: Schweizerische Mineralogische und Petrogrographische Mitteilungen, v. 75, p. 187–199.

MANUSCRIPT RECEIVED BY THE SOCIETY NOVEMBER 10, 1995
REVISED MANUSCRIPT RECEIVED APRIL 26, 1996
MANUSCRIPT ACCEPTED JULY 8, 1996
Printed in U.S.A.